

Theory of diffraction: dipole model and diffractive pdfs

Anna Staśto



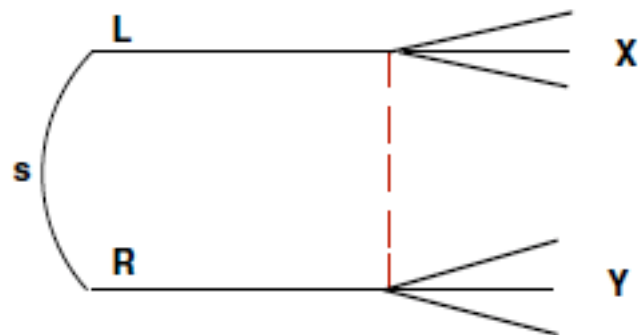
Outline

- Inclusive diffraction in DIS
- Diffractive PDFs
- Limits on collinear factorization at low x
- Twist expansion and dipole model
- VM production and impact parameter-dependence
- Questions for theory and for experiment

Diffractive processes

Diffractive processes are characterized by the rapidity gap: absence of any activity in part of the detector

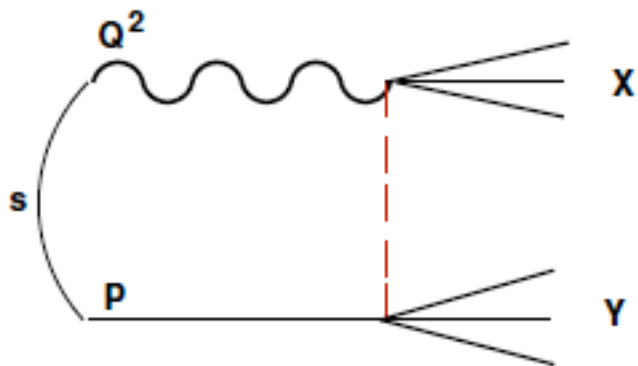
Hadron-hadron



Single diffractive dissociation SD
Double diffractive dissociation DD
Elastic scattering

$$s \gg |t|, M_X^2, M_Y^2$$

Deep Inelastic Scattering



$$s \gg Q^2, |t|, M_p^2$$

semihard process:

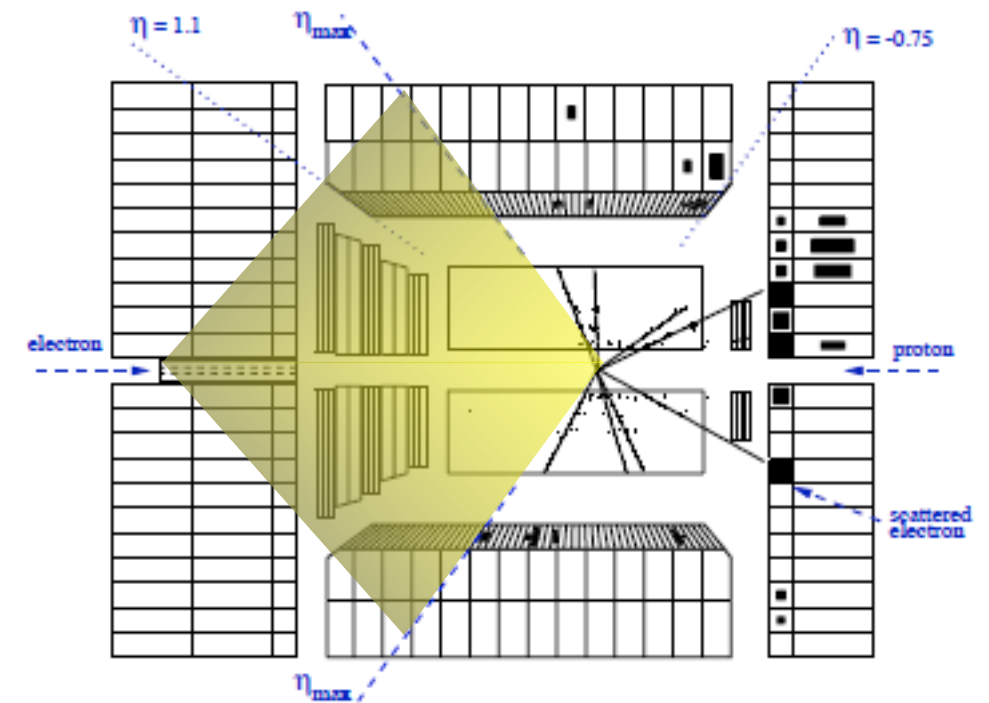
$$\Lambda_{QCD}^2 \ll Q^2 \ll s$$

perturbative QCD applicable

Diffraction: thought to be mediated by the exchange of 'object' with vacuum quantum numbers - the Pomeron

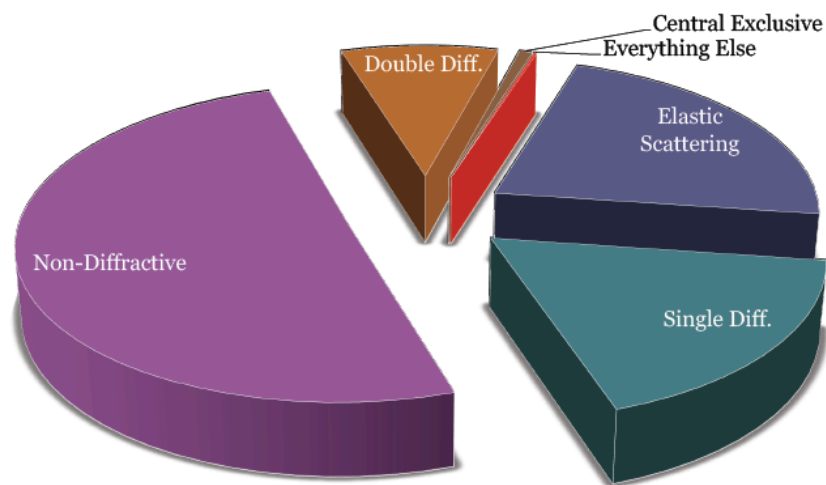
How often such events occur at high energies?

At HERA (electron -proton collisions): 10% diffractive



Diffractive event in ZEUS

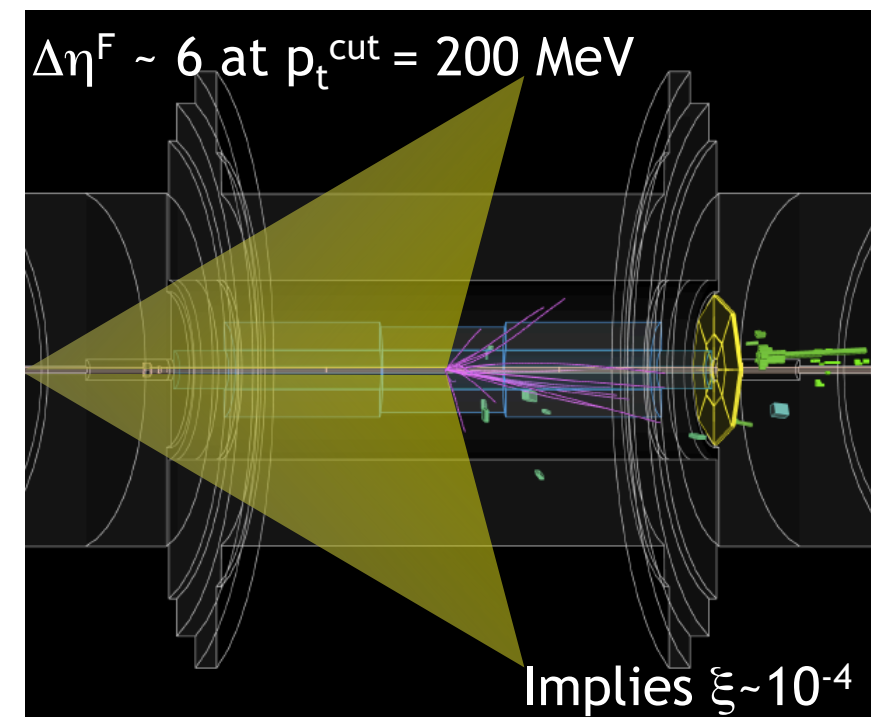
At LHC:



25% elastic: both protons intact

25% diffractive: rapidity gap

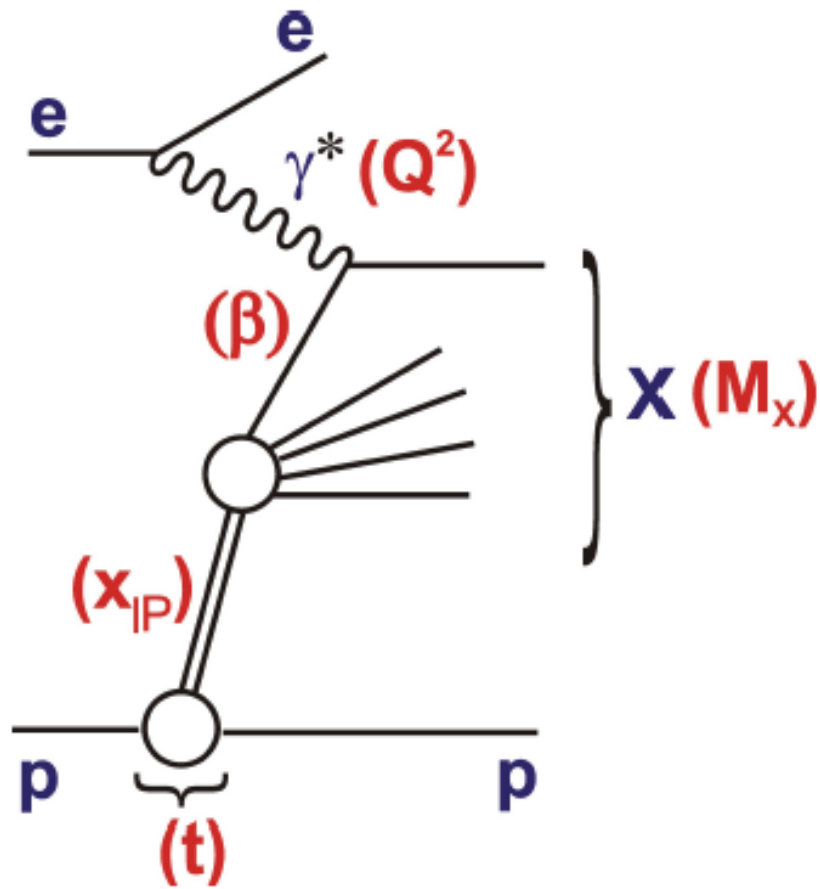
Very large number of these quasi-elastic events!



Diffractive event in ATLAS

Diffractive kinematics in DIS

Standard DIS variables:



electron-proton
cms energy squared:

$$s = (k + p)^2$$

photon-proton
cms energy squared:

$$W^2 = (q + p)^2$$

inelasticity

$$y = \frac{p \cdot q}{p \cdot k}$$

Bjorken x

$$x = \frac{-q^2}{2p \cdot q}$$

(minus) photon virtuality

$$Q^2 = -q^2$$

Diffractive DIS variables:

$$x_{IP} = \frac{Q^2 + M_X^2 - t}{Q^2 + W^2}$$

momentum fraction of
the Pomeron w.r.t hadron

$$\beta = \frac{Q^2}{Q^2 + M_X^2 - t}$$

momentum fraction of
parton w.r.t Pomeron

$$x_{Bj} = x_{IP} \beta$$

$$t = (p - p')^2$$

4-momentum transfer squared

Two classes of diffractive events in DIS:

$$Q^2 \sim 0$$

photoproduction

$$Q^2 \gg 0$$

deep inelastic scattering

Diffractive structure functions

$$\frac{d^3\sigma^D}{dx_{IP} dx dQ^2} = \frac{2\pi\alpha_{\text{em}}^2}{xQ^4} Y_+ \sigma_r^{D(3)}(x_{IP}, x, Q^2)$$

$$Y_+ = 1 + (1 - y)^2$$

Reduced diffractive cross section depends on two structure functions

$$\sigma_r^{D(3)} = F_2^{D(3)} - \frac{y^2}{Y_+} F_L^{D(3)}$$

For y not too close to unity we have:

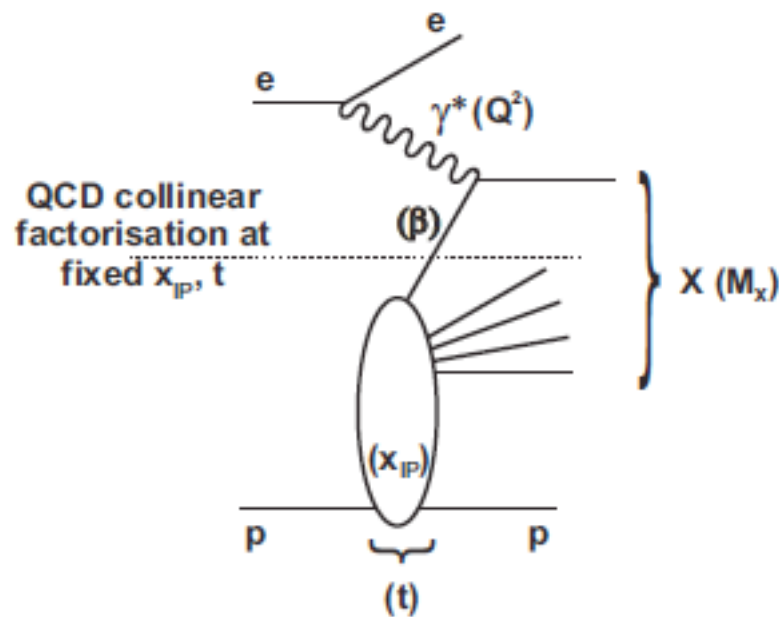
$$\sigma_r^{D(3)} \simeq F_2^{D(3)}$$

Integrated vs unintegrated structure functions over t

$$F_{T,L}^{D(3)}(x, Q^2, x_{IP}) = \int_{-\infty}^0 dt F_{T,L}^{D(4)}(x, Q^2, x_{IP}, t)$$

$$F_2^{D(4)} = F_T^{D(4)} + F_L^{D(4)}$$

Collinear factorization in diffraction



Collins

Collinear factorization in diffractive DIS

$$d\sigma^{ep \rightarrow eXY}(x, Q^2, x_{IP}, t) = \sum_i f_i^D(x, Q^2, x_{IP}, t) \otimes d\hat{\sigma}^{ei}(x, Q^2) + \mathcal{O}(\Lambda^2/Q^2)$$

- Diffractive cross section can be factorized into the convolution of the perturbatively calculable partonic cross sections and diffractive parton distributions (DPDFs).
- Partonic cross sections are the same as for the inclusive DIS.
- The DPDFs represent the probability distributions for partons i in the proton under the constraint that the proton is scattered into the system Y with a specified 4-momentum.
- Factorization should be valid for sufficiently(?) large Q^2 (and fixed t and x_{IP}).
- Another way of asking the same question: what is value of Λ ?

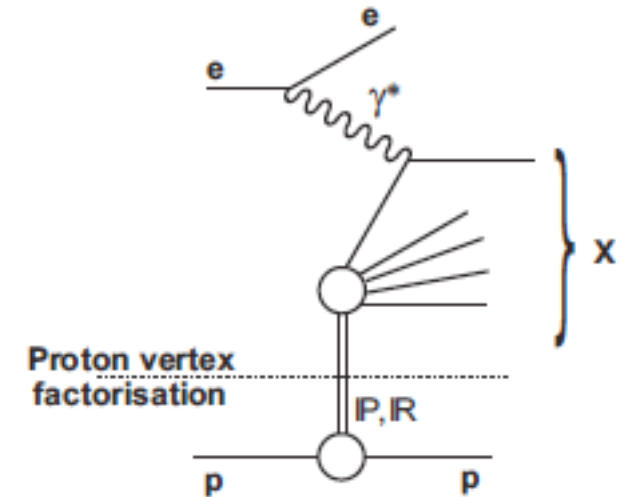
Regge factorization

Ingelman-Schlein model:

$$f_i^D(x, Q^2, x_{IP}, t) = f_{IP/p}(x_{IP}, t) f_i(\beta = x/x_{IP}, Q^2)$$

pomeron flux

parton distributions in the
pomeron



- It is usually assumed that Regge vertex factorization occurs.
- This is in addition to collinear factorization. It is a different assumption.
- The diffractive scattering occurs through the exchange of the Pomeron with the longitudinal momentum fraction x_{IP} of the proton.
- The Pomeron couples to the proton through the 'pomeron flux factor' that determines probability of the coupling with particular value of x_{IP} and t .
- Subsequent hard scattering of the photon on a partonic constituents of the Pomeron. The struck parton carries fraction β of the longitudinal momentum of the Pomeron.

DPDF parametrization

Example of parametrization by H1 and ZEUS:

Standard choice of parametrization similar to the inclusive PDFs:

$$f_k(z) = A_k x^{B_k} (1 - x)^{C_k}$$

where k=g,d. Light quarks assumed to be equal u=d=s.

Pomeron flux is parametrized as

$$f_{IP/p}(x_{IP}, t) = A_{IP} \frac{e^{B_{IP} t}}{x^{2\alpha_{IP}(t)-1}}$$

Pomeron trajectory assumed to be linear:

$$\alpha_{IP}(t) = \alpha_{IP}(0) + \alpha'_{IP} t$$

For good description of the data usually subleading Reggeons are included

$$f_i^D(x, Q^2, x_{IP}, t) = f_{IP/p}(x_{IP}, t) f_i(\beta, Q^2) + n_{IR} f_{IR/p}(x_{IP}, t) f_i^{IR}(\beta, Q^2)$$

Subleading contributions important for large values of $x_{IP} > 0.01$

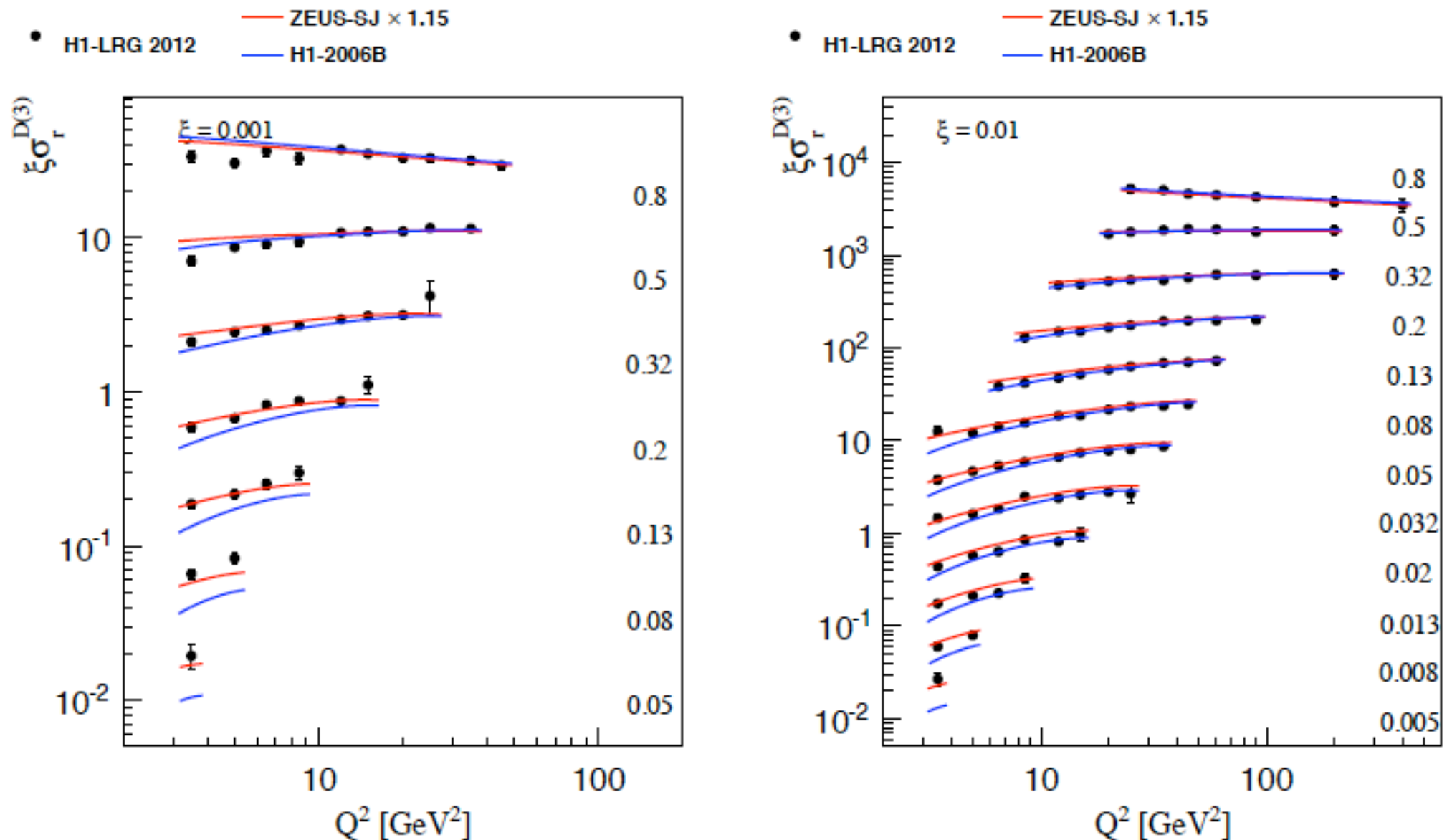
Reggeon parton distributions are constrained by the data on the pion structure functions.

Diffractive fits

Example of the DGLAP fit to the diffractive data

$$\xi = x_{IP}$$

plot by W.Slominski



Comparison of H1-2006B and ZEUS-SJ fits to the H1-LRG 2012 data
ZEUS-SJ fit seems to better describe the data in the low β region

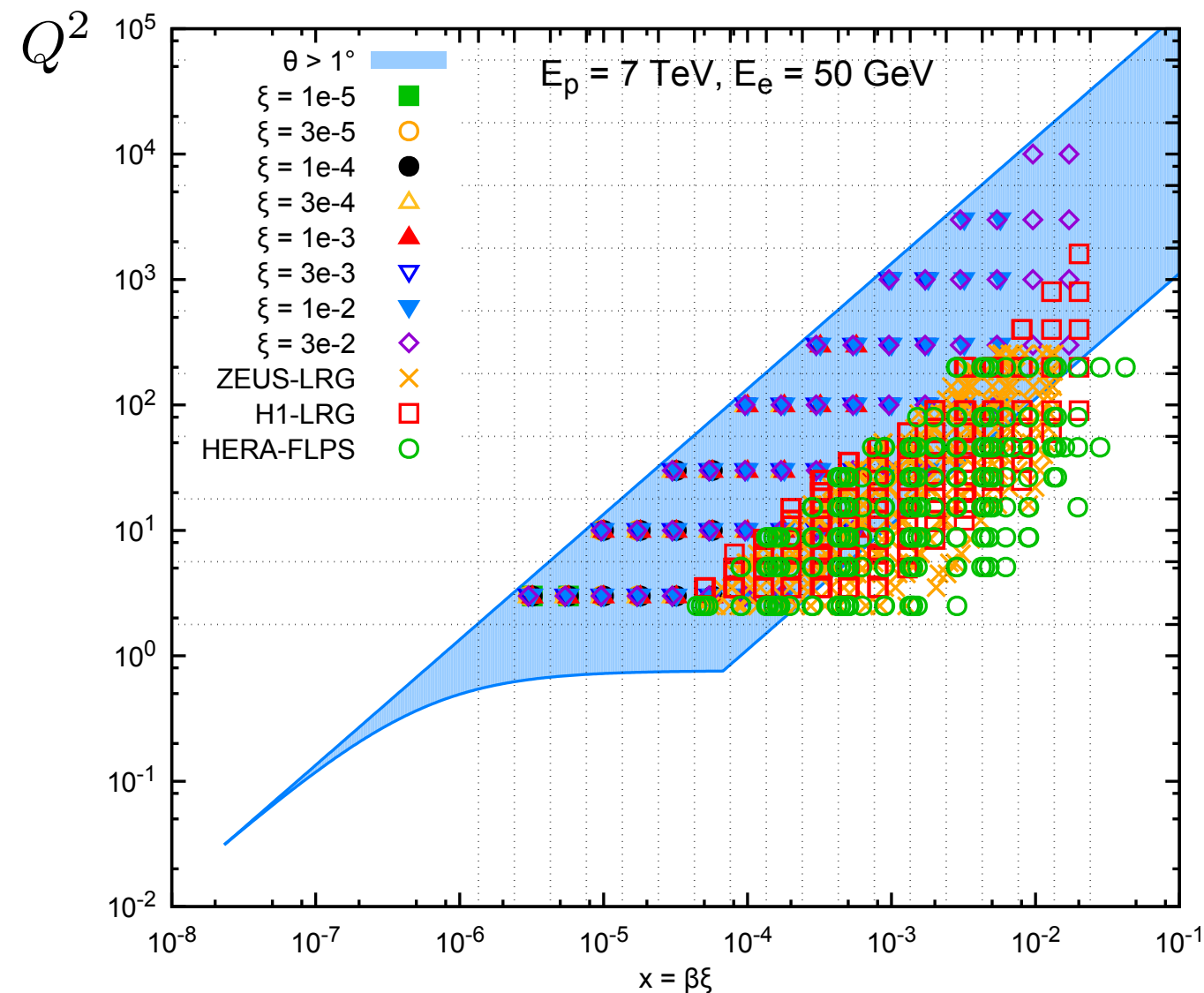
Diffractive structure functions: prospects

What can be done/tested in the future generation electron-proton(ion) collider?

- Testing proton vertex factorization; where does it work? Does it break down and where?
- Extended kinematics (eg. LHeC).
- Limits on factorization? Higher twists.
- DPDFs for nuclei.

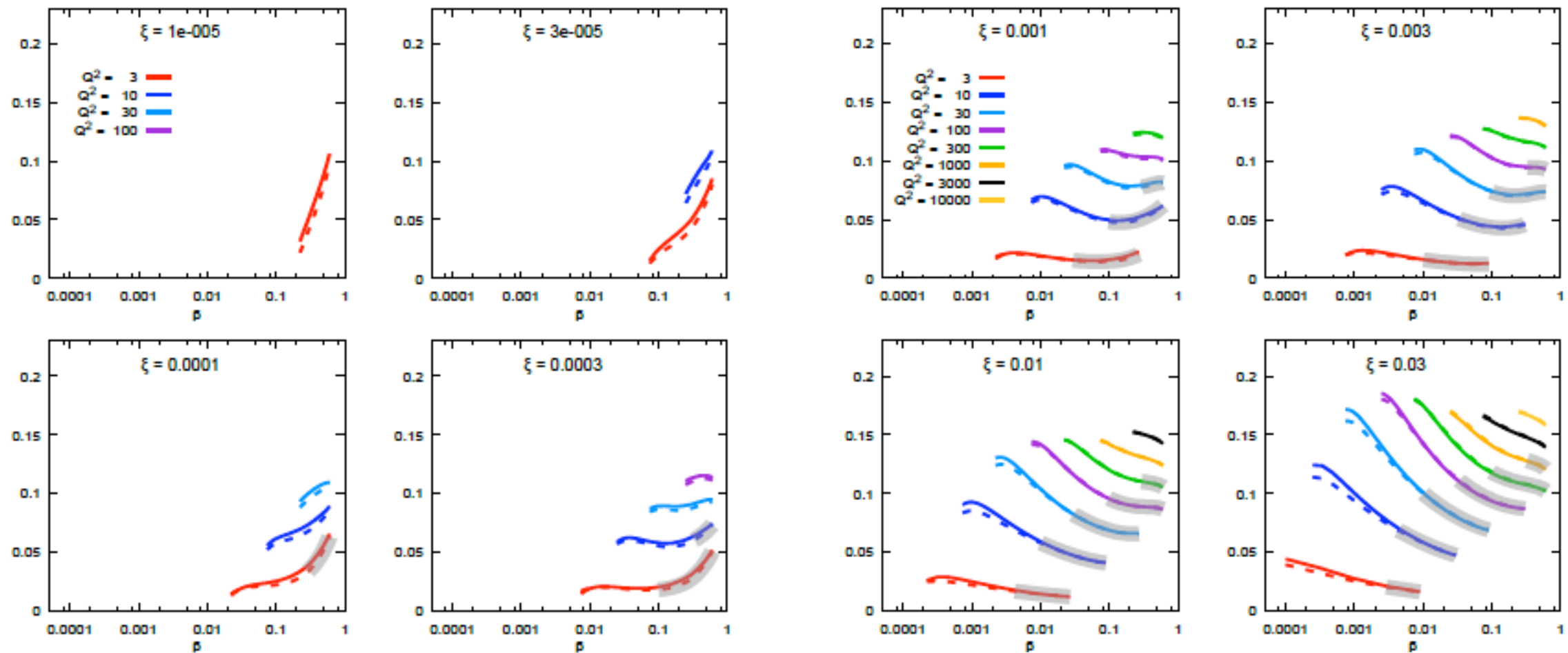
Example: Kinematic range for diffraction at LHeC

preliminary LHeC study by W.Slominski



Diffractive structure functions: prospects

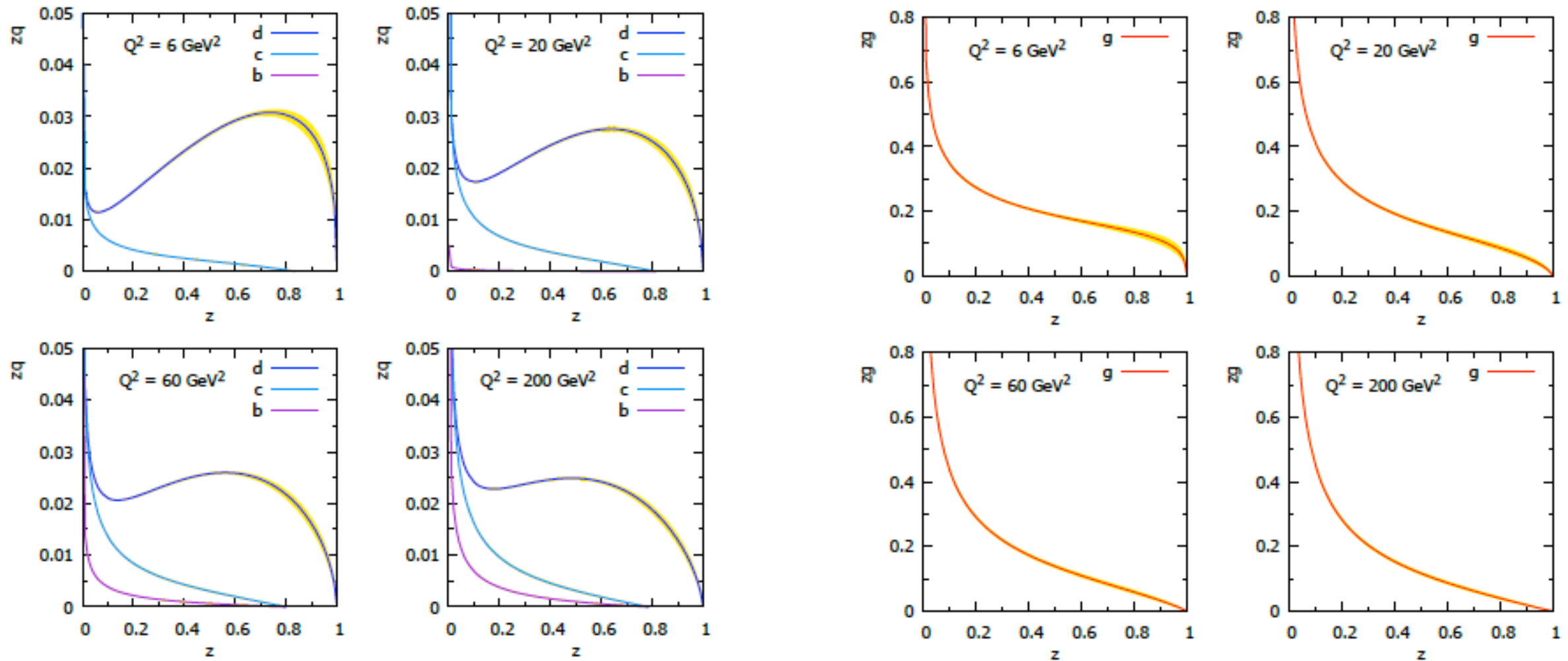
Reduced cross section extrapolated beyond HERA range (grey bands) with two different fits.



preliminary LHeC study by W.Slominski

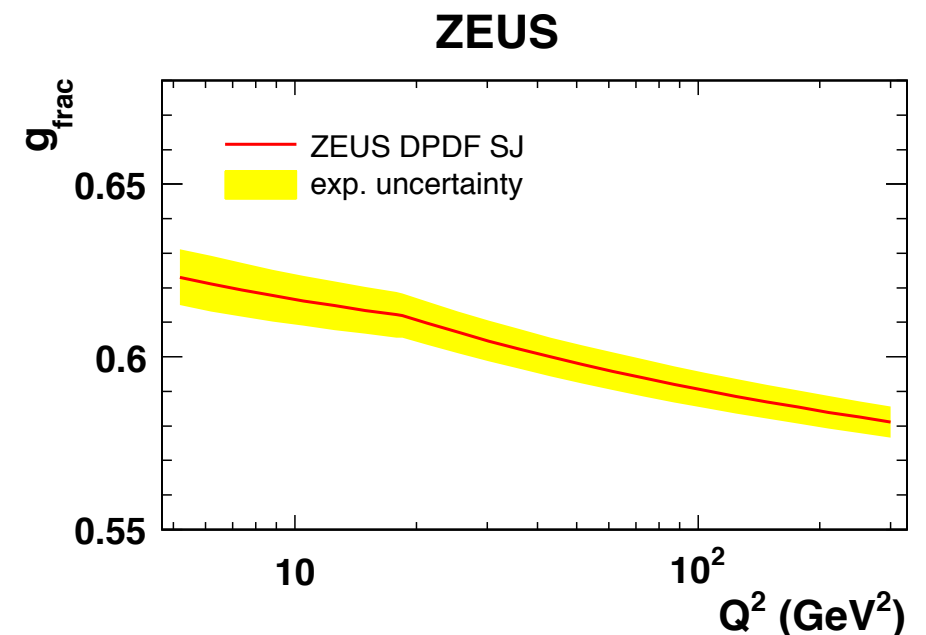
- Fits start to differ beyond HERA range.
- Possibility of constraining the gluon content of the Pomeron using LHeC.

Diffractive pdfs: prospects



preliminary LHeC study by W.Slominski

DPDFs extracted from fits to the diffractive structure functions using simulated LHeC data and assuming 5% error. Very small uncertainty on the distributions, can significantly improve over the HERA data.



Limits on collinear factorization

In general twist-2 factorization valid for sufficiently large values of Q^2 .

Big question: how low Q^2 until it breaks down, i.e. higher twists become important?

$$d\sigma^{ep \rightarrow eXY}(x, Q^2, x_{IP}, t) = \sum_i f_i^D(x, Q^2, x_{IP}, t) \otimes d\hat{\sigma}^{ei}(x, Q^2) + \mathcal{O}(\Lambda^2/Q^2)$$

Eg. in inclusive DIS:

$$W^{\mu\nu} = \sum_{\tau} \left(\frac{\Lambda}{Q}\right)^{\tau-2} \sum_i C_{\tau,i}^{\mu\nu} \otimes f_{\tau,i}(Q^2/\Lambda^2)$$

- Higher twists are suppressed by powers of hard scale.
- Theoretically are related to the evolution of quasipartonic operators (for which twist equals the number of partons in the t-channel).
- Formal analysis difficult; more information in the low x limit.
- Relation to multiple scattering, saturation, parton correlations.

Dipole model of DIS: high energy limit of QCD which allows to conveniently include corrections due to parton saturation (i.e. higher twists)

Higher twist analysis within dipole model

Phenomenological analyses which estimate the value of higher twists in different processes, some using GBW or QCD improved Glauber model (with parton saturation):

- Inclusive DIS: Bartels, Golec-Biernat, Peters; Bartels, Golec-Biernat, Motyka; Motyka, Sadzikowski, Slominski, Wichmann; Abt, Cooper-Sarkar, Foster, Myronenko, Wichmann, Wing
- Forward Drell-Yan: Golec-Biernat, Lewandowska, AS; Motyka, Sadzikowski, Stebel
- Diffraction DIS: Motyka, Sadzikowski, Slominski

Recap of dipole model in DIS

Cross section:

$$\sigma_{T,L}^{\gamma^*p}(x, Q^2) = \sum_f \int d^2\mathbf{r} \int_0^1 dz |\Psi_{T,L}^f(z, r, Q^2)|^2 \sigma(x, \mathbf{r})$$

Photon wave function (lowest order):

$$|\Psi_T^f(z, r, Q^2)|^2 = \frac{2N_c\alpha_{em}e_f^2}{4\pi^2} \{ [z^2 + (1-z)^2] \epsilon^2 K_1^2(\epsilon r) + m_f^2 K_0^2(\epsilon r) \}$$

$$|\Psi_L^f(z, r, Q^2)|^2 = \frac{8N_c\alpha_{em}e_f^2}{4\pi^2} Q^2 z^2 (1-z)^2 K_0^2(\epsilon r)$$

$$\epsilon^2 = z(1-z)Q^2 + m_f^2$$

Cross section vs structure function:

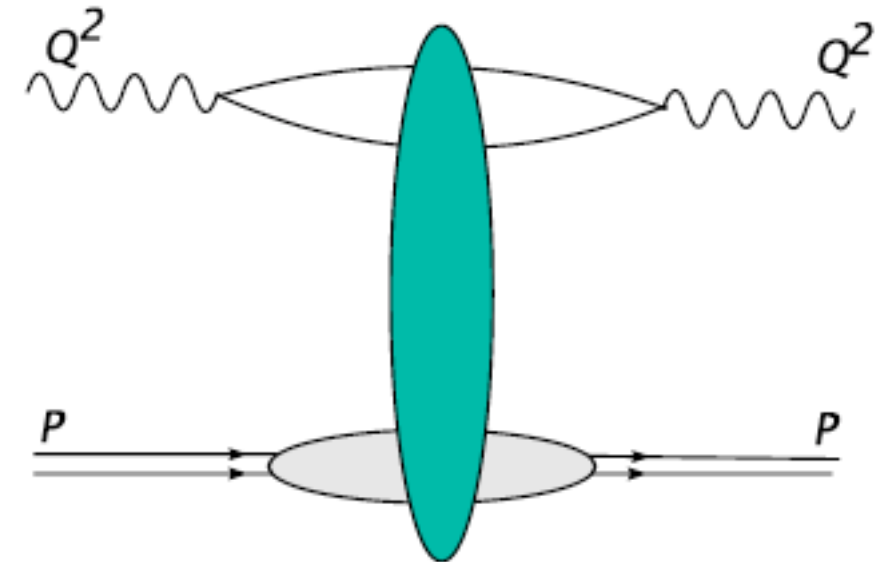
$$\sigma_{T,L}(x, Q^2) = \frac{4\pi^2\alpha_{em}}{Q^2} F_{T,L}(x, Q^2)$$

GBW model:

$$\sigma(x, \mathbf{r}) = \sigma_0 [1 - \exp(-r^2 Q_s^2(x))]$$

Saturation scale:

$$Q_s(x)^2 = Q_0^2 x^{-\lambda}$$



Dipole cross section:

$$\sigma(x, \mathbf{r})$$

Contains all the information about the interaction with the target

Twist analysis in dipole model

Twist expansion is performed using the Mellin space

$$\sigma_{T,L}^{\gamma^*p}(x, Q^2) = \int_0^\infty \frac{dr^2}{r^2} H_{T,L}(r, Q^2) \sigma(x, r) \quad H_{T,L}(r, Q^2) \equiv \pi r^2 \sum_f \int_0^1 dz |\Psi_{T,L}^f(z, r, Q^2)|^2$$

Mellin representation

$$\sigma(x, r) = \int_C \frac{ds}{2\pi i} (r^2 Q_0^2)^{-s} \tilde{\sigma}(x, s)$$

$$\sigma_{L,T}^{\gamma^*p}(x, Q^2) = \int_{C_s} \frac{ds}{2\pi i} \left(\frac{Q_0^2}{Q^2} \right)^{-s} \tilde{\sigma}(x, s) \tilde{H}_{T,L}(-s)$$

For GBW model it leads to simple analytic answer:

$$\begin{aligned} \tilde{\sigma}(x, s) &= \sigma_0 \int_0^\infty dr^2 (r^2)^{s-1} \{1 - \exp(-r^2 Q_{\text{sat}}^2(x)/4)\} \\ &= -\sigma_0 \left(\frac{Q_{\text{sat}}^2}{4} \right)^{-s} \Gamma(s). \end{aligned}$$

Singularities in Mellin space: poles in the dipole cross section multiplied by the poles in the photon impact factor: give analytic twist decomposition of the model with saturation

$$\sigma_{L,T}^{\gamma^*p}(x, Q^2) = \sigma_0 \int_{C_s} \frac{ds}{2\pi i} \left(\frac{Q_{\text{sat}}^2}{Q^2} \right)^{-s} \{-\Gamma(s)\} \tilde{H}_{T,L}(-s)$$

Since model has geometric scaling the expansion is in terms of Q_{sat}^2/Q^2

Twist analysis in dipole model

Original GBW model: simple analytic answer proportional to powers of Q_{sat}^2/Q^2

$$\sigma_{T,L}^{(\tau=2n)} = \sigma_0 \frac{Q_{\text{sat}}^{2n}}{Q^{2n}} \left\{ -\gamma_1^{(n)} a_{T,L}^{(n)} \log(Q^2/Q_{\text{sat}}^2) + \left(\gamma_1^{(n)} b_{T,L}^{(n)} - \gamma_0^{(n)} a_{T,L}^{(n)} \right) \right\}$$

(enhanced by the logarithmic corrections originating from double poles)

twist 2

$$\sigma_T^{(\tau=2)} = \frac{\alpha_{em}\sigma_0}{\pi} \langle e^2 \rangle \frac{Q_{\text{sat}}^2}{Q^2} \{ \log(Q^2/Q_{\text{sat}}^2) + \gamma_E + 1/6 \}$$

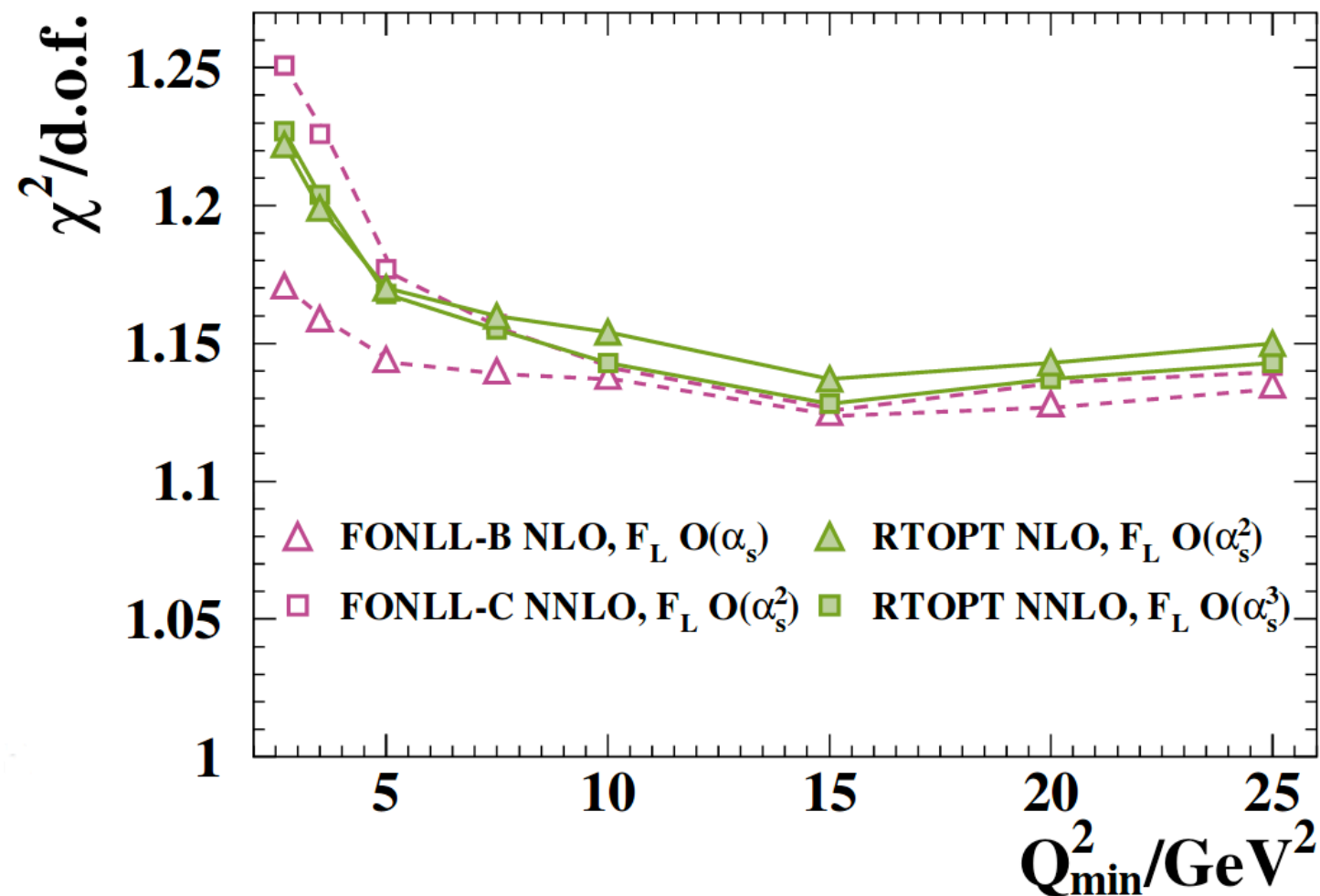
$$\sigma_L^{(\tau=2)} = \frac{\alpha_{em}\sigma_0}{\pi} \langle e^2 \rangle \frac{Q_{\text{sat}}^2}{Q^2}$$

twist 4

$$\sigma_T^{(\tau=4)} = \frac{3}{5} \frac{\alpha_{em}\sigma_0}{\pi} \langle e^2 \rangle \frac{Q_{\text{sat}}^4}{Q^4}$$

$$\sigma_L^{(\tau=4)} = -\frac{4}{5} \frac{\alpha_{em}\sigma_0}{\pi} \langle e^2 \rangle \frac{Q_{\text{sat}}^4}{Q^4} \{ \log(Q^2/Q_{\text{sat}}^2) + \gamma_E + 1/15 \}$$

Global fit of combined HERA data



Test of DGLAP

description quality:

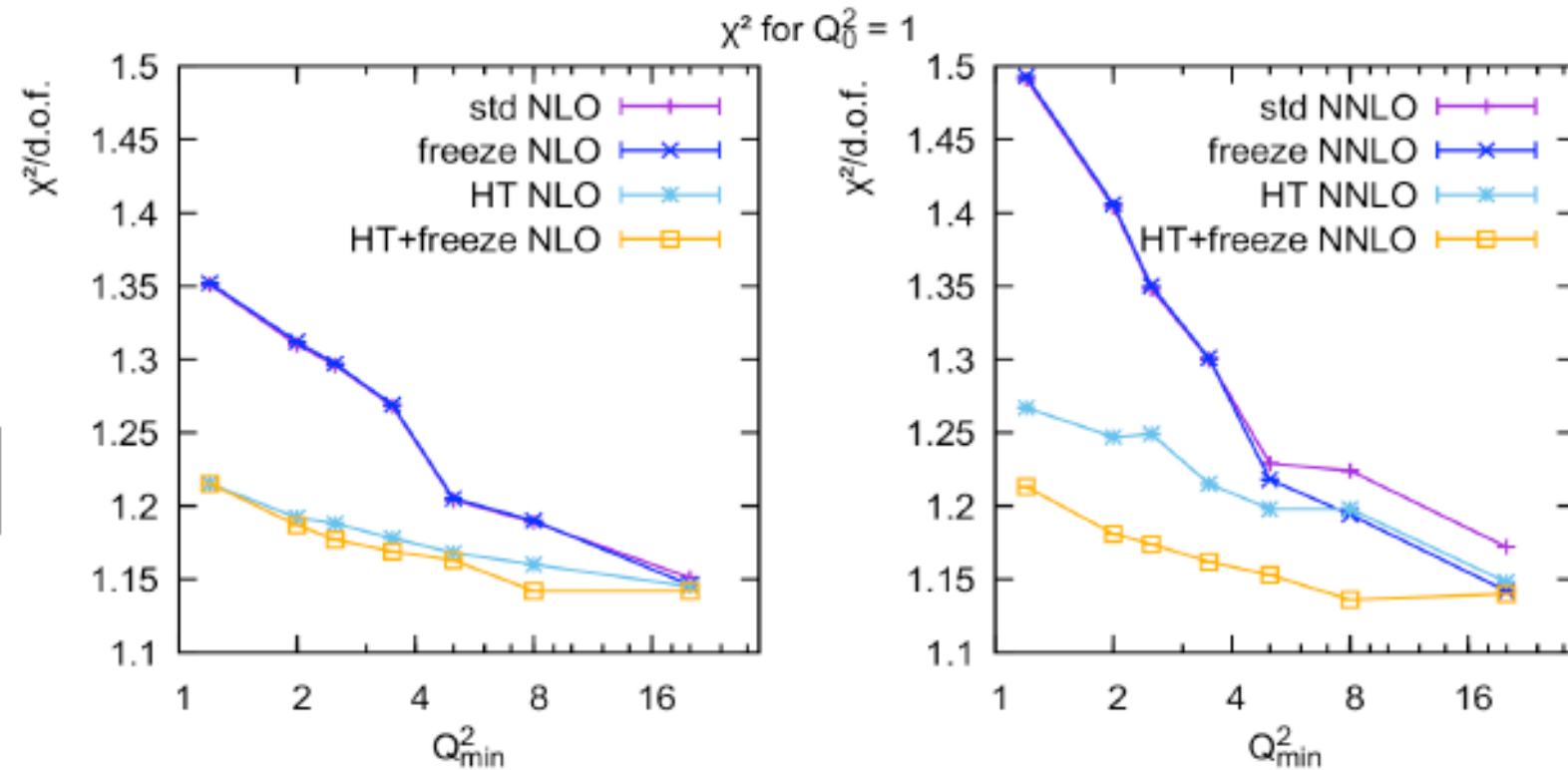
- start evolution from Q_0
($Q_0^2 = 1.9 \text{ GeV}^2$)
- cut the data $Q^2 > Q_{\min}^2$,
fit and compute χ^2
- check variation of
 $\chi^2/\text{d.o.f.}$ as function of Q_{\min}^2
- **found: deterioration of DGLAP fits quality below $\sim 5 \text{ GeV}^2$**

Indication of higher twists in inclusive data?

talk by L.Motyka at DIS2017

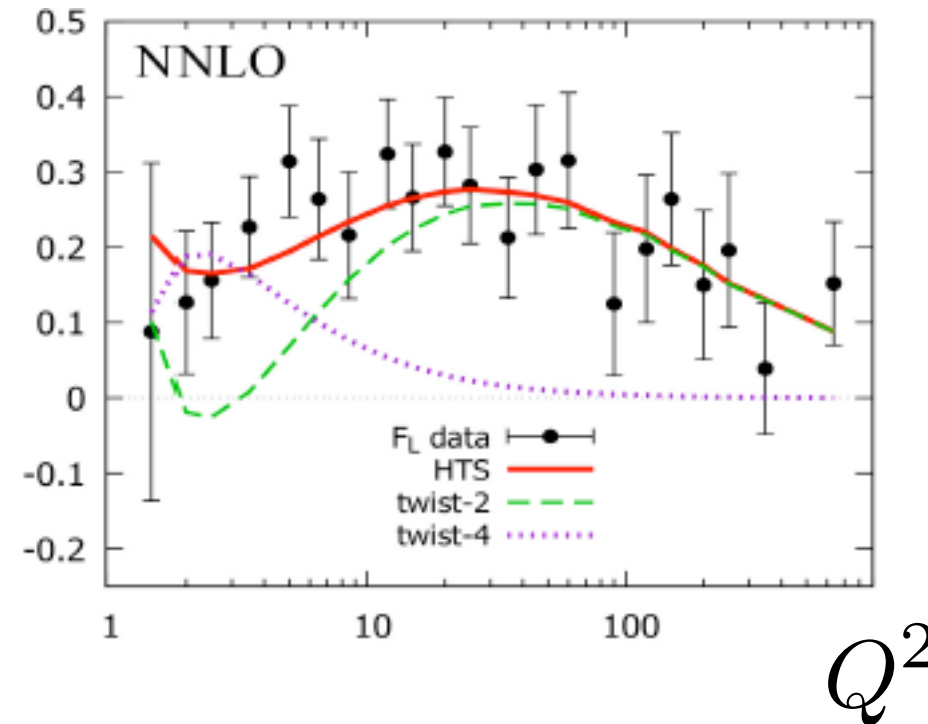
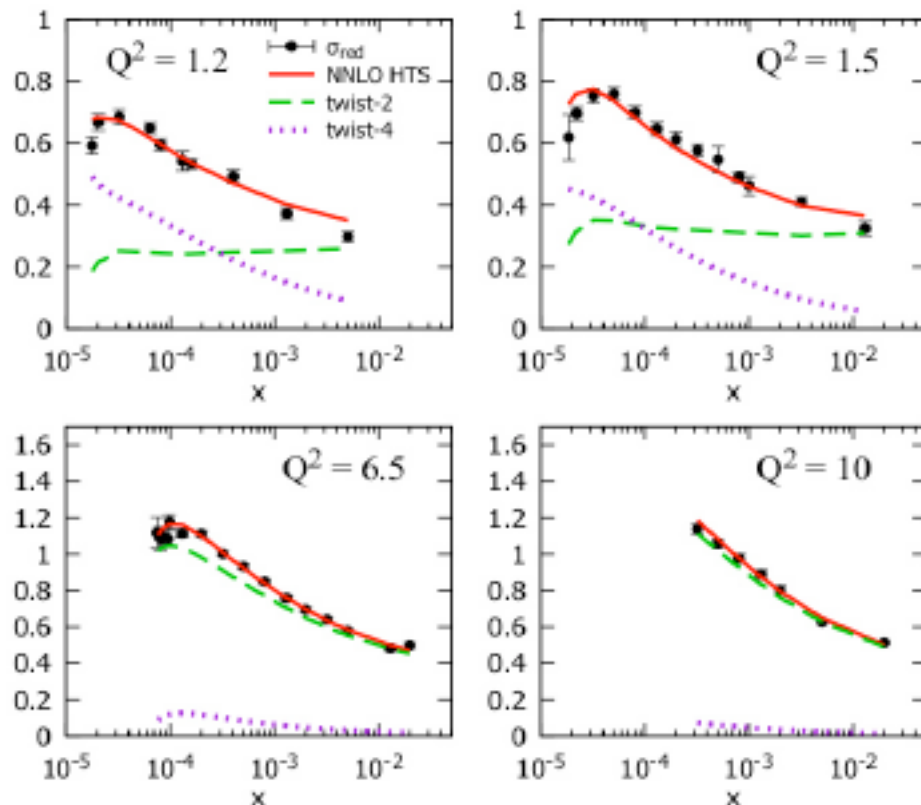
DGLAP fits with twist-4 parametrization

$$F_{T/L}^{(\tau=4)} = \frac{Q_0^2(x)}{Q^2} x^{-2\lambda} \left[c_{T/L}^{(0)} + c_{T/L}^{(log)} \left(\log \frac{Q_0^2}{Q^2} + \lambda \log \frac{1}{x} \right) \right]$$



At low Q^2 : HT may be 40%

significant improvement of the fit quality



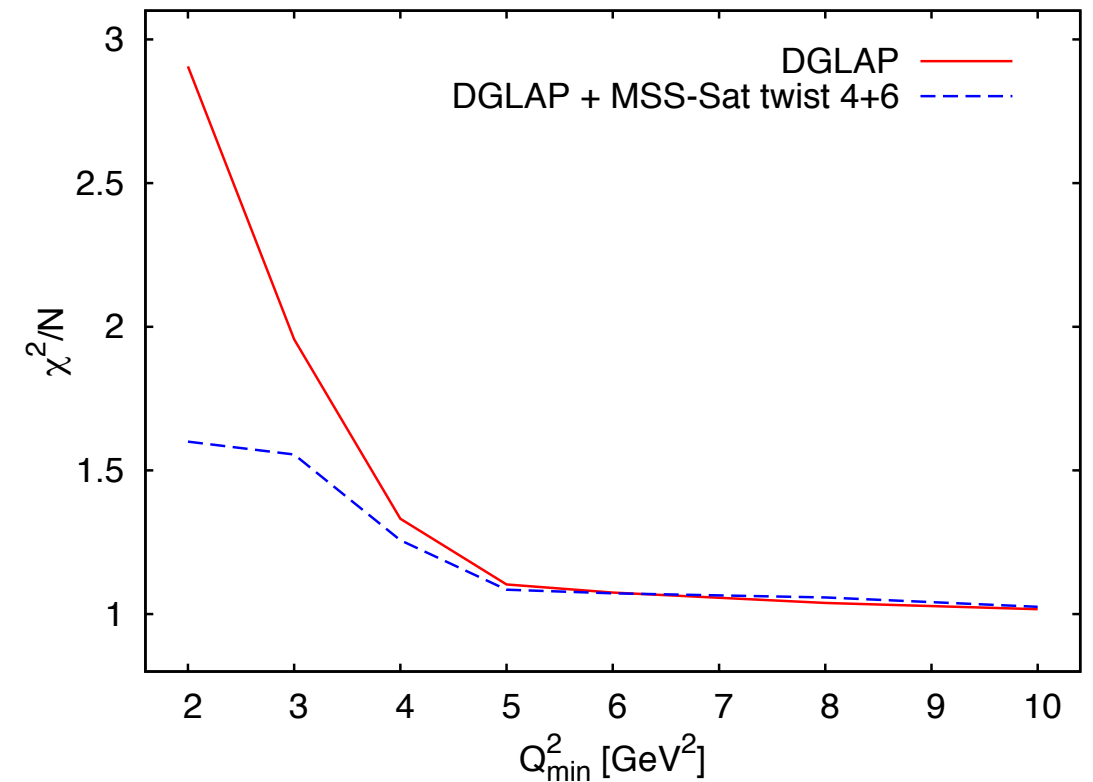
- Good description of F_L down to lowest Q^2
- Large contribution of HT below 10 GeV^2

What about higher twists in diffraction?

DGLAP fits have problem describing diffractive data at low values of $Q^2 < 5 \text{ GeV}^2$

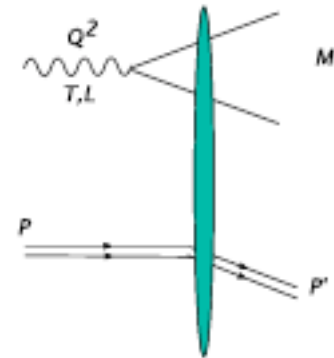
Indication of higher twists in diffraction?

Dipole model description of diffraction:



Motyka, Sadzikowski, Slominski

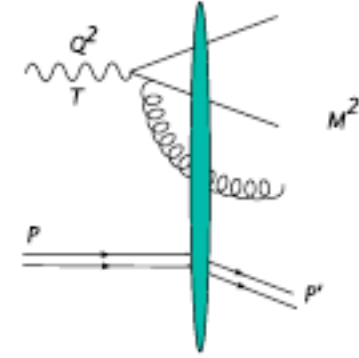
quark-antiquark component



$$\frac{d\sigma_{L,T}^{q\bar{q}}}{dM_X^2} = \frac{1}{16\pi b_D} \int \frac{d^2p}{(2\pi)^2} \int_0^1 dz \delta\left(\frac{p^2}{z\bar{z}} - M_x^2\right) \sum_f \sum_{spin} \left| \int d^2r e^{i\vec{p}\cdot\vec{r}} \psi_{h\bar{h},\lambda}^f(Q, z, \vec{r}) \sigma_d(r, \xi) \right|^2$$

Higher twists in diffraction

In addition quark-antiquark-gluon component is needed as well



$$\frac{d\sigma_{L,T}^{q\bar{q}g}}{dM_x^2} = \frac{1}{16\pi b_D} \frac{N_c \alpha_s}{2\pi^2} \frac{\sigma_0^2}{M_x^2} \int d^2 r_{01} N_{q\bar{q}g}^2(r_{01}, \xi) \sum_f \sum_{spin} \int_0^1 dz |\psi_{h\bar{h},\lambda}^f(Q, z, r_{01})|^2,$$

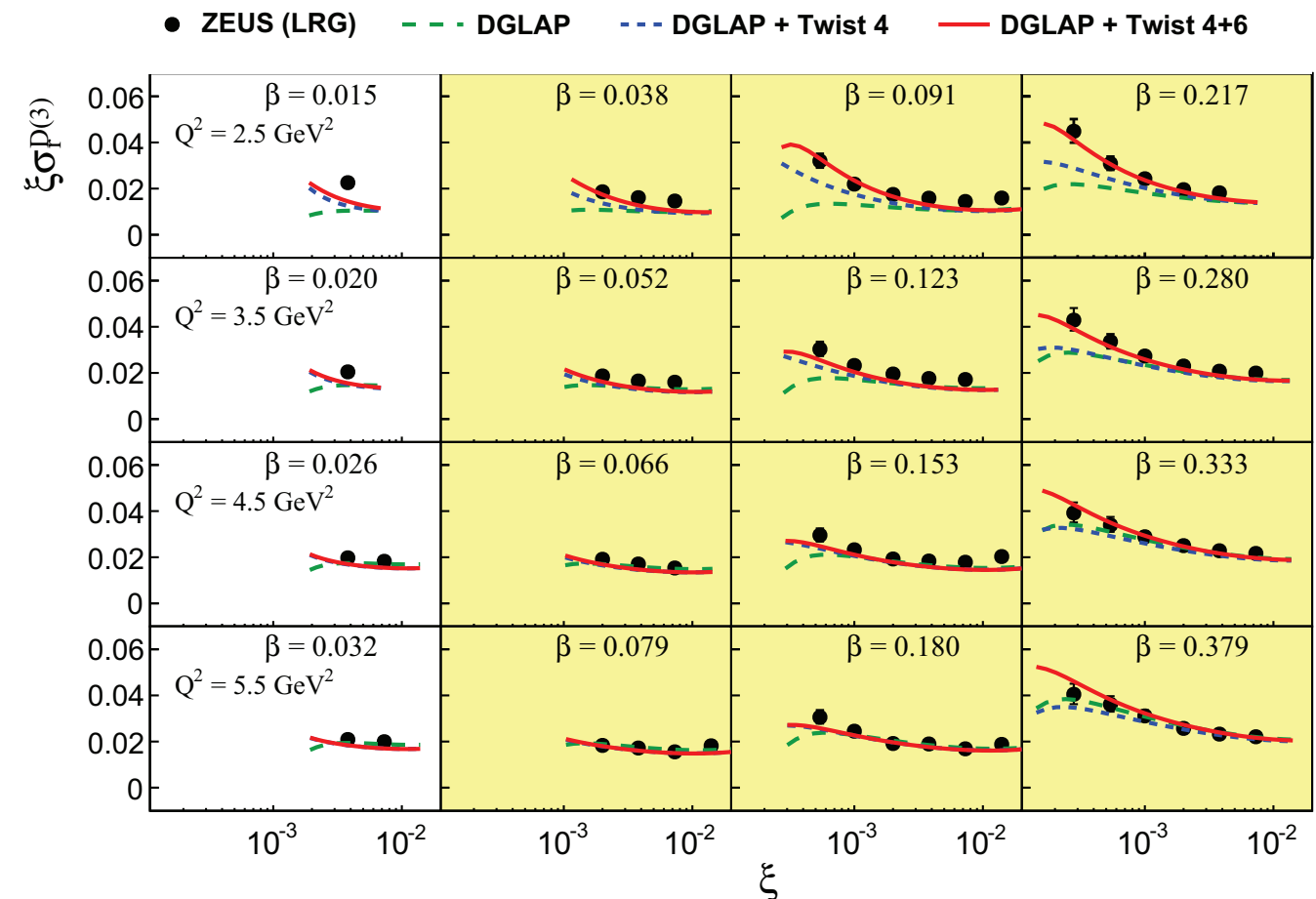
$$N_{q\bar{q}g}^2(r_{01}) = \int d^2 r_{02} \frac{r_{01}^2}{r_{02}^2 r_{12}^2} (N_{02} + N_{12} - N_{02}N_{12} - N_{01})^2$$

$$N_{ij} = N(\vec{r}_j - \vec{r}_i), \vec{r}_{01}, \vec{r}_{02}, \vec{r}_{12} = \vec{r}_{02} - \vec{r}_{01}$$

Using Mellin transform can extract higher twist contribution (exactly in the GBW model)

Combination of DGLAP and twist 4 and 6 describes data much better than pure DGLAP in the low Q region

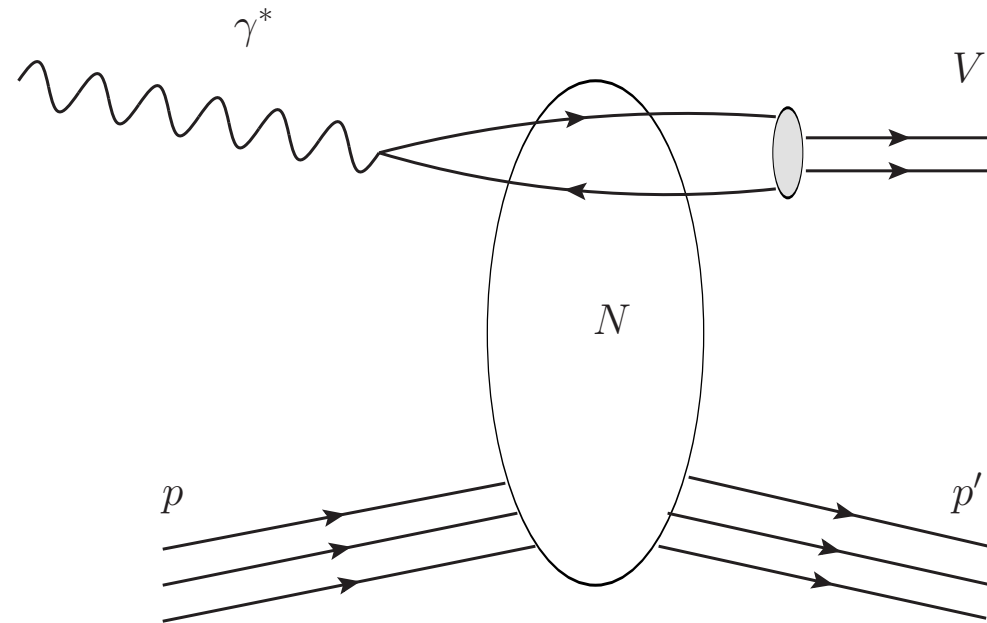
Motyka, Sadzikowski, Slominski



Exclusive production of vector mesons in the dipole approach

Nikolaev,Zkharov;
Strikman, Frankfurt, Rogers;
Levin et al;
Munier, Mueller, AS;
Motyka, Kowalski, Watt;
Berger, AS;
Armesto, Rezaeian;
Lappi, Mantysaari, Schenke;...

$\rho, \Phi, J/\psi, \Upsilon$ production



cross section

$$\frac{d\sigma}{dt} = \frac{1}{16\pi} |A(x, \Delta, Q)|^2$$

amplitude

$$A(x, \Delta, Q) = \sum_{h, \bar{h}} \int d^2\mathbf{r} \int dz \Psi_{h, h^*}(\mathbf{r}, z, Q^2) \mathcal{N}(x, \mathbf{r}, \Delta) \Psi_{\bar{h}, \bar{h}^*}^V(\mathbf{r}, z)$$

dipole cross section

$$\sigma_{\text{dip}}(x, \mathbf{r}) = \text{Im } i\mathcal{N}(x, \mathbf{r}, \Delta = 0)$$

dipole amplitude

$$\mathcal{N}(x, \mathbf{r}, \Delta) = 2 \int d^2\mathbf{b} N(x, \mathbf{r}, \mathbf{b}) e^{i\Delta \cdot \mathbf{b}}$$

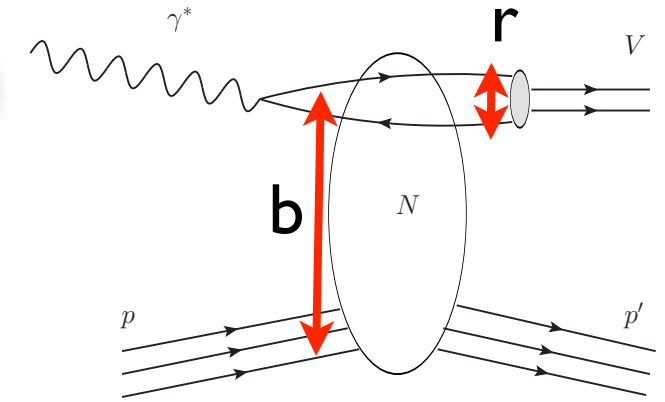
\mathbf{r} dipole size

\mathbf{b} impact parameter

Δ momentum transfer

$z, (1 - z)$ fraction of the longitudinal momentum of the photon carried by the quark(anti-quark)

Low x dipole amplitude: including saturation



Glauber-Mueller parameterization often used; includes nonlinear effects

Motyka, Kowalski, Watt; 'b-Sat model'

$$N_{\text{GM}}(r, b; Y = \ln 1/x) = 1 - \exp \left(-\frac{\pi^2}{2N_c} r^2 x g(x, \eta^2) T(b) \right)$$

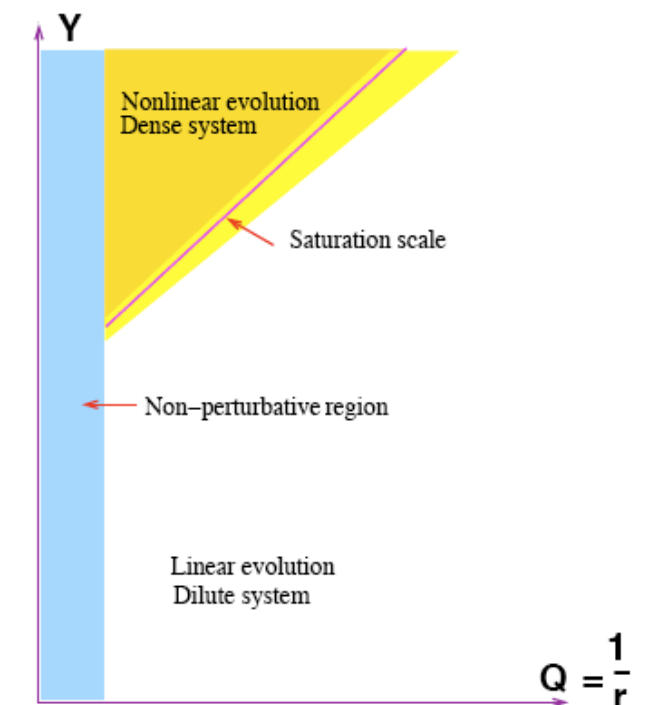
$$T(b) = \frac{1}{8\pi} e^{\frac{-b^2}{2B_G}}$$

Can be obtained from low x nonlinear equation: Balitsky - Kovchegov equation

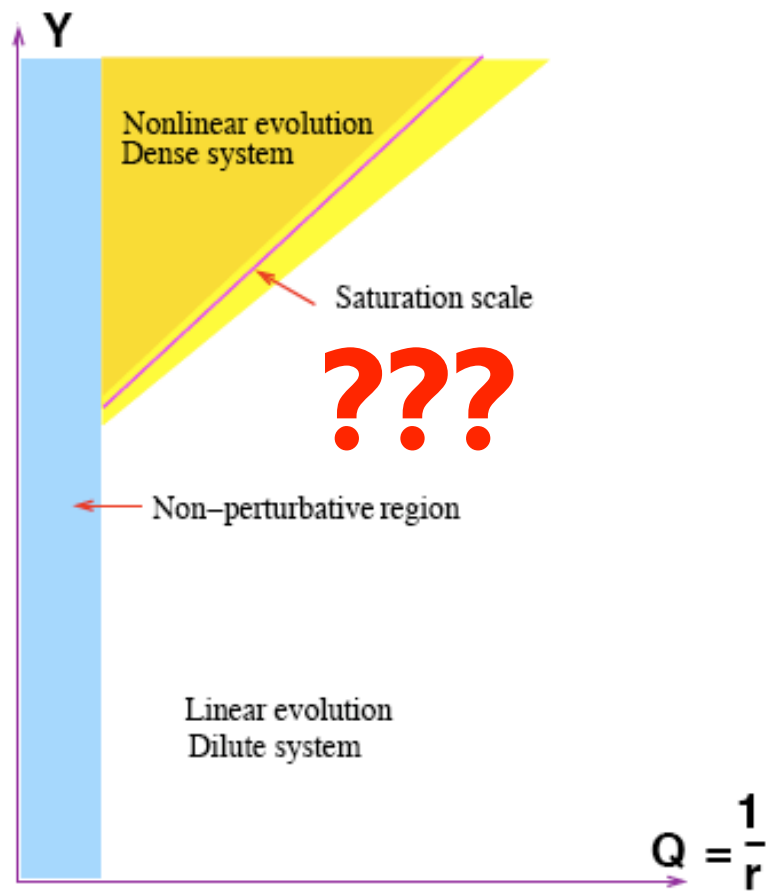
Berger, AS

$$\begin{aligned} \frac{dN(\mathbf{r}_{01}, \mathbf{b}_{01}, Y)}{dY} = & \frac{\alpha_s N_c}{\pi} \int \frac{d^2 \mathbf{r}_2 \mathbf{r}_{01}^2}{\mathbf{r}_{20}^2 \mathbf{r}_{12}^2} \left[N(\mathbf{r}_{20}, \mathbf{b}_{01} + \frac{\mathbf{r}_{12}}{2}, Y) + N(\mathbf{r}_{12}, \mathbf{b}_{01} - \frac{\mathbf{r}_{20}}{2}, Y) \right. \\ & \left. - N(\mathbf{r}_{01}, \mathbf{b}_{01}, Y) - N(\mathbf{r}_{20}, \mathbf{b}_{01} + \frac{\mathbf{r}_{12}}{2}, Y) N(\mathbf{r}_{12}, \mathbf{b}_{01} - \frac{\mathbf{r}_{20}}{2}, Y) \right] \end{aligned}$$

- Typically BK solved in a local approximation: without impact parameter dependence. Successful description of variety of data.
- Can be solved (at least numerically) relatively easily.
- Generates the saturation scale that divides the dense and dilute regime.



What about spatial distribution?



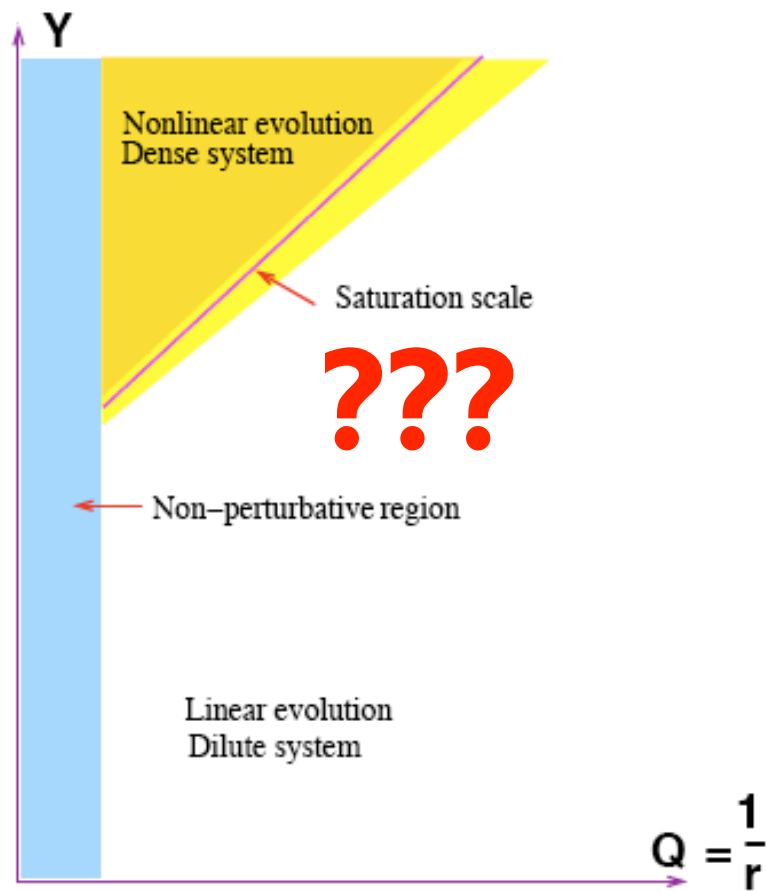
Usual approximation:

$$N(\mathbf{r}, \mathbf{b}, Y) = N(\mathbf{r}, Y)$$

- The target has infinite size.
- Local approximation suggests that the system becomes more perturbative as the energy grows.
- But this cannot be true everywhere (IR in QCD)

Impact parameter profile

What about spatial distribution?

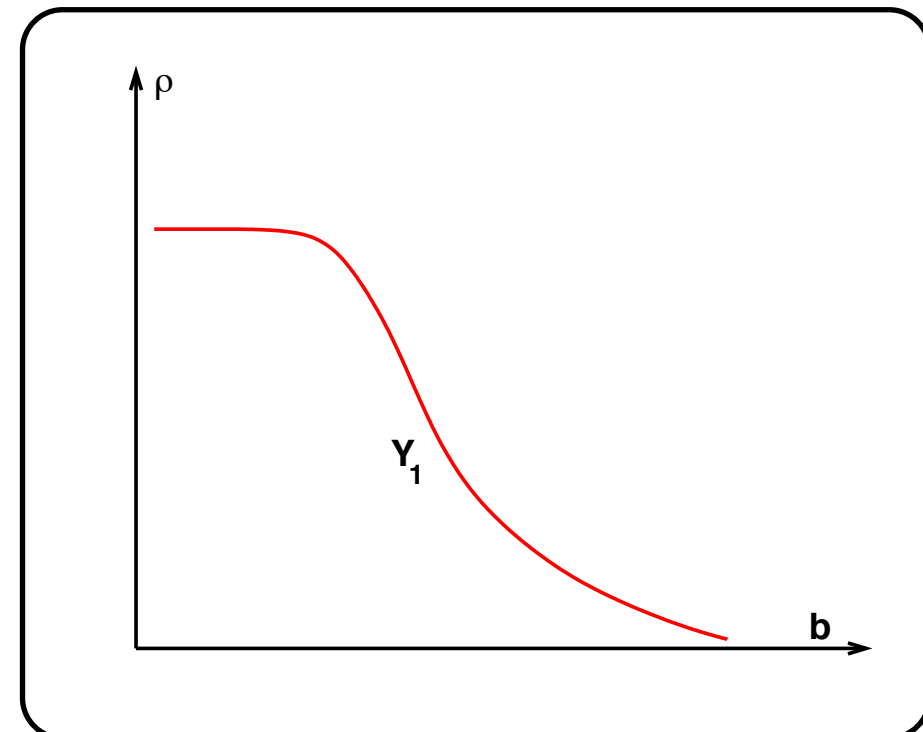
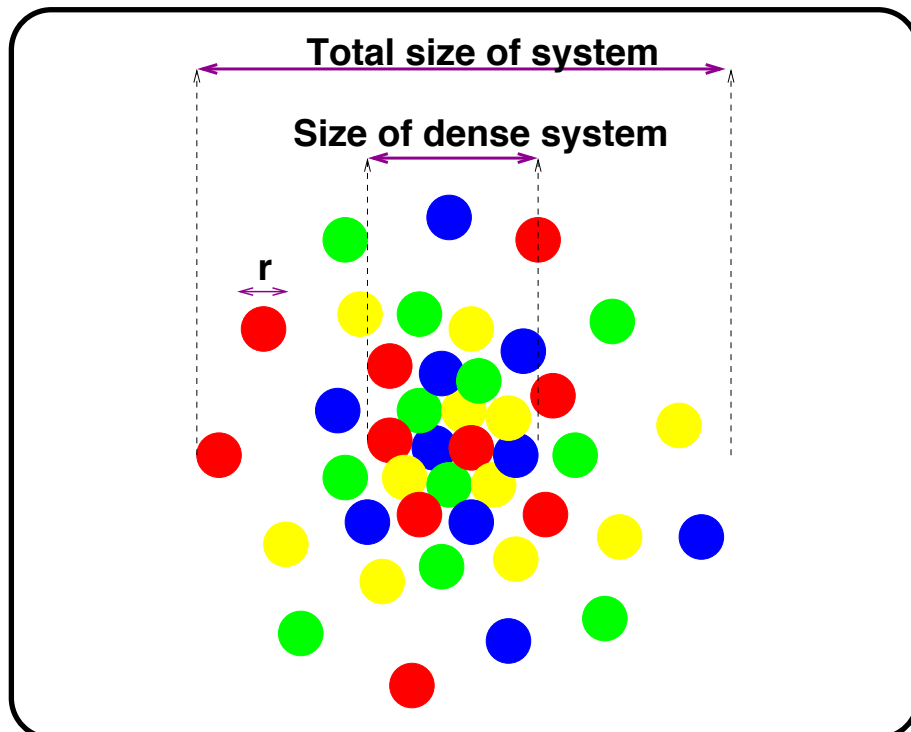


Usual approximation:

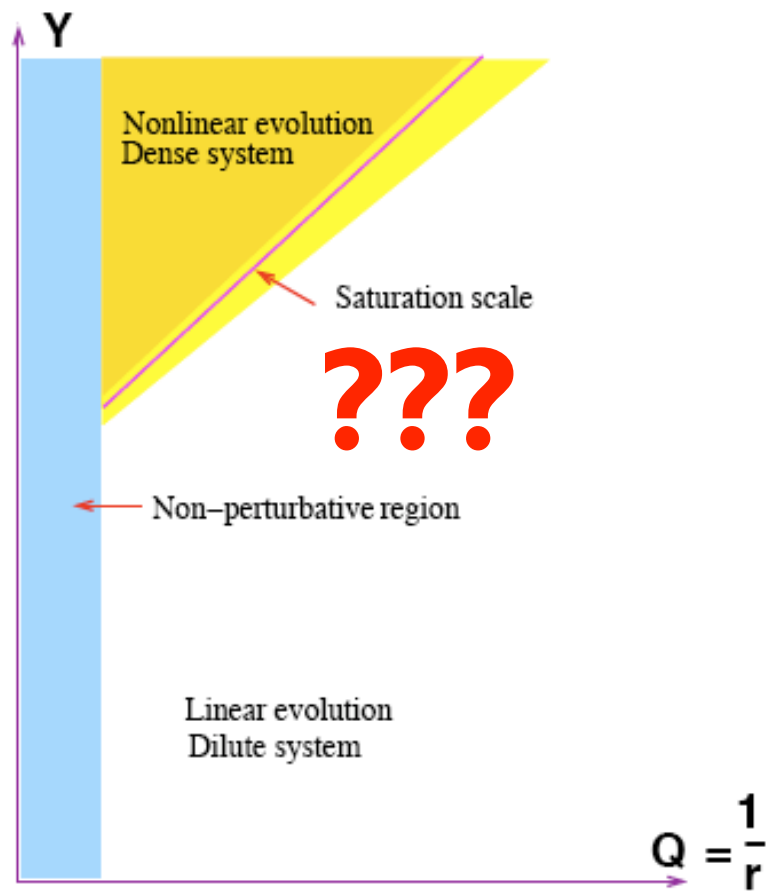
$$N(\mathbf{r}, \mathbf{b}, Y) = N(\mathbf{r}, Y)$$

- The target has infinite size.
- Local approximation suggests that the system becomes more perturbative as the energy grows.
- But this cannot be true everywhere (IR in QCD)

Impact parameter profile



What about spatial distribution?

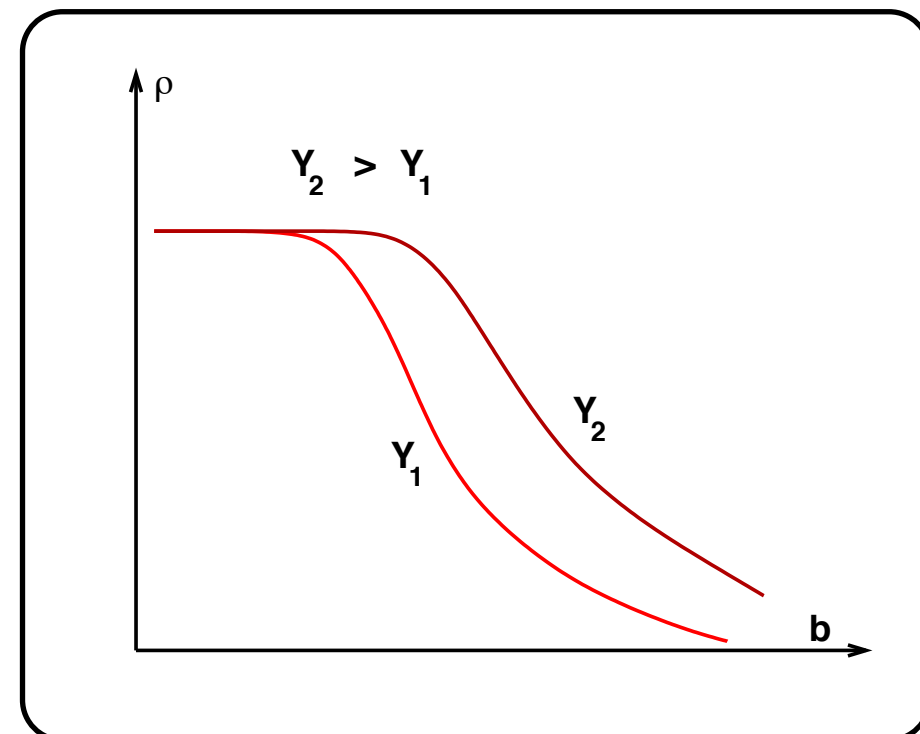
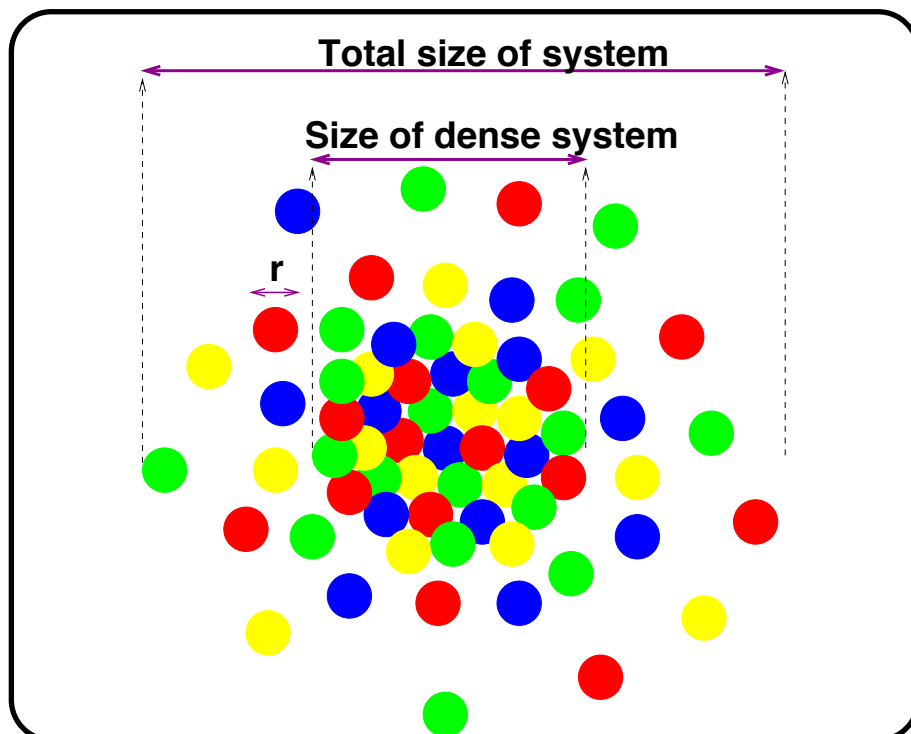


Usual approximation:

$$N(\mathbf{r}, \mathbf{b}, Y) = N(\mathbf{r}, Y)$$

- The target has infinite size.
- Local approximation suggests that the system becomes more perturbative as the energy grows.
- But this cannot be true everywhere (IR in QCD)

Impact parameter profile



Solving impact parameter dependent BK equation

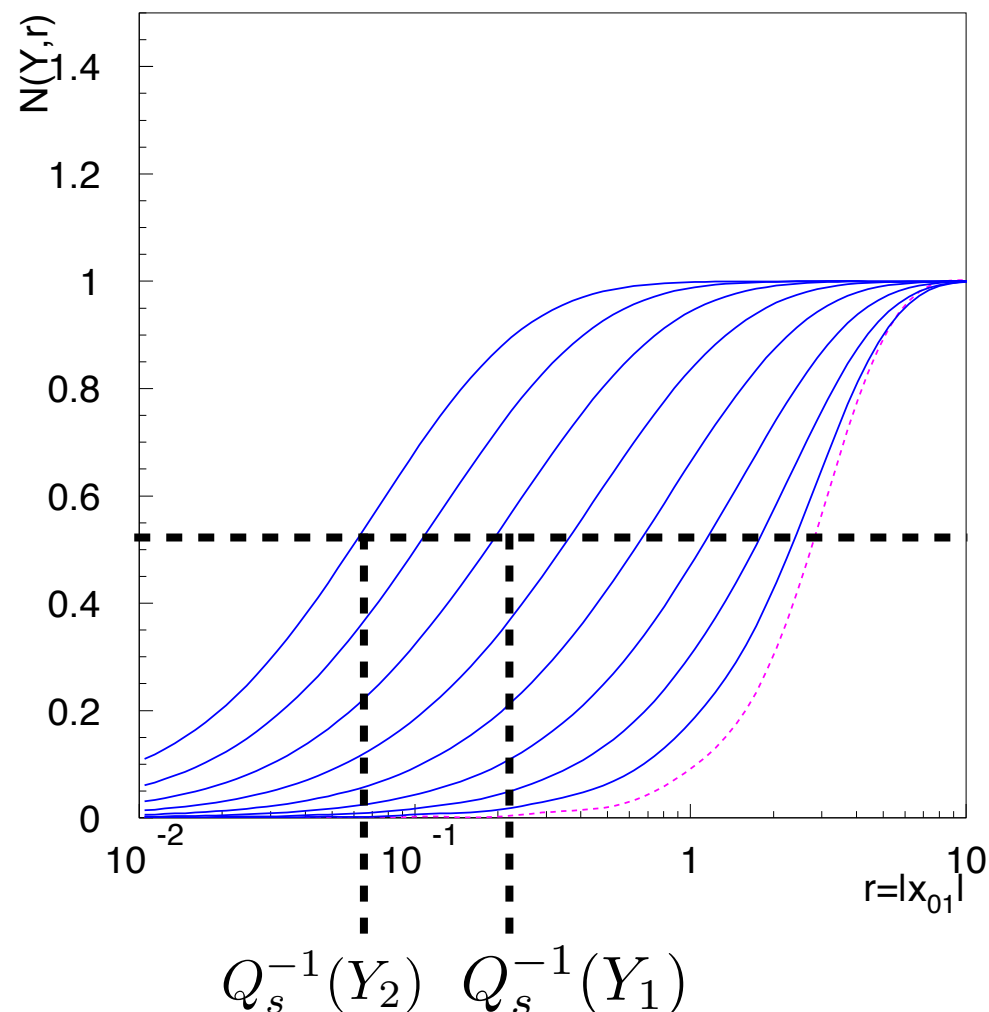
$$\frac{dN(\mathbf{r}_{01}, \mathbf{b}_{01}, Y)}{dY} = \frac{\alpha_s N_c}{\pi} \int \frac{d^2 \mathbf{r}_2 d^2 \mathbf{r}_{01}}{\mathbf{r}_{20}^2 \mathbf{r}_{12}^2} \left[N(\mathbf{r}_{20}, \mathbf{b}_{01} + \frac{\mathbf{r}_{12}}{2}, Y) + N(\mathbf{r}_{12}, \mathbf{b}_{01} - \frac{\mathbf{r}_{20}}{2}, Y) \right. \\ \left. - N(\mathbf{r}_{01}, \mathbf{b}_{01}, Y) - N(\mathbf{r}_{20}, \mathbf{b}_{01} + \frac{\mathbf{r}_{12}}{2}, Y) N(\mathbf{r}_{12}, \mathbf{b}_{01} - \frac{\mathbf{r}_{20}}{2}, Y) \right]$$

Golec-
Biernat,AS;
Berger,AS;

Initial condition Glauber-Mueller type: $N^{(0)} = 1 - \exp(-c_r r^2 \exp(-c_b b^2))$

Without impact parameter dependence

Dipole amplitude as a function of dipole size(arbitrary units)



Golec-Biernat,AS

Solving impact parameter dependent BK equation

$$\frac{dN(\mathbf{r}_{01}, \mathbf{b}_{01}, Y)}{dY} = \frac{\alpha_s N_c}{\pi} \int \frac{d^2 \mathbf{r}_2 \mathbf{r}_{01}^2}{\mathbf{r}_{20}^2 \mathbf{r}_{12}^2} \left[N(\mathbf{r}_{20}, \mathbf{b}_{01} + \frac{\mathbf{r}_{12}}{2}, Y) + N(\mathbf{r}_{12}, \mathbf{b}_{01} - \frac{\mathbf{r}_{20}}{2}, Y) \right. \\ \left. - N(\mathbf{r}_{01}, \mathbf{b}_{01}, Y) - N(\mathbf{r}_{20}, \mathbf{b}_{01} + \frac{\mathbf{r}_{12}}{2}, Y) N(\mathbf{r}_{12}, \mathbf{b}_{01} - \frac{\mathbf{r}_{20}}{2}, Y) \right]$$

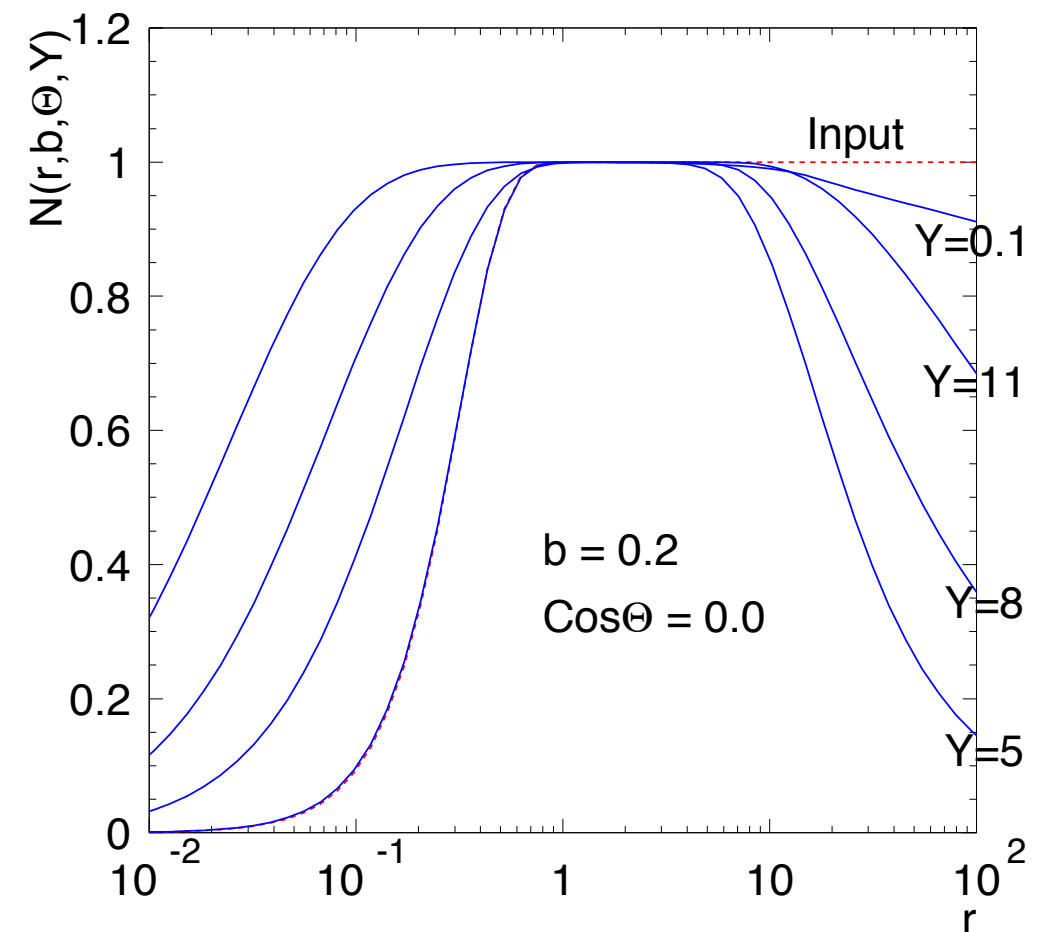
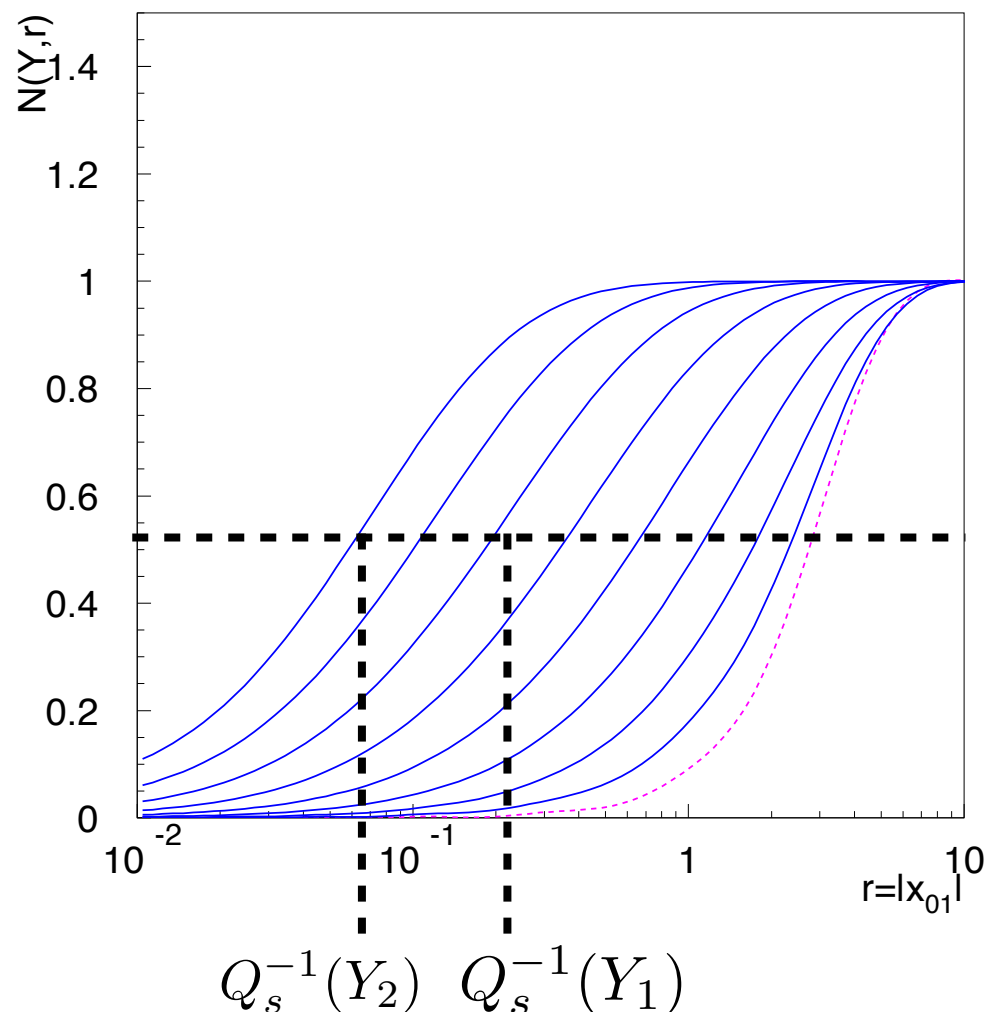
Golec-
Biernat,AS;
Berger,AS;

Initial condition Glauber-Mueller type: $N^{(0)} = 1 - \exp(-c_r r^2 \exp(-c_b b^2))$

Without impact parameter dependence

With impact parameter dependence

Dipole amplitude as a function of dipole size(arbitrary units)



Golec-Biernat,AS

Solving impact parameter dependent BK equation

$$\frac{dN(\mathbf{r}_{01}, \mathbf{b}_{01}, Y)}{dY} = \frac{\alpha_s N_c}{\pi} \int \frac{d^2 \mathbf{r}_2 \mathbf{r}_{01}^2}{\mathbf{r}_{20}^2 \mathbf{r}_{12}^2} \left[N(\mathbf{r}_{20}, \mathbf{b}_{01} + \frac{\mathbf{r}_{12}}{2}, Y) + N(\mathbf{r}_{12}, \mathbf{b}_{01} - \frac{\mathbf{r}_{20}}{2}, Y) \right. \\ \left. - N(\mathbf{r}_{01}, \mathbf{b}_{01}, Y) - N(\mathbf{r}_{20}, \mathbf{b}_{01} + \frac{\mathbf{r}_{12}}{2}, Y) N(\mathbf{r}_{12}, \mathbf{b}_{01} - \frac{\mathbf{r}_{20}}{2}, Y) \right]$$

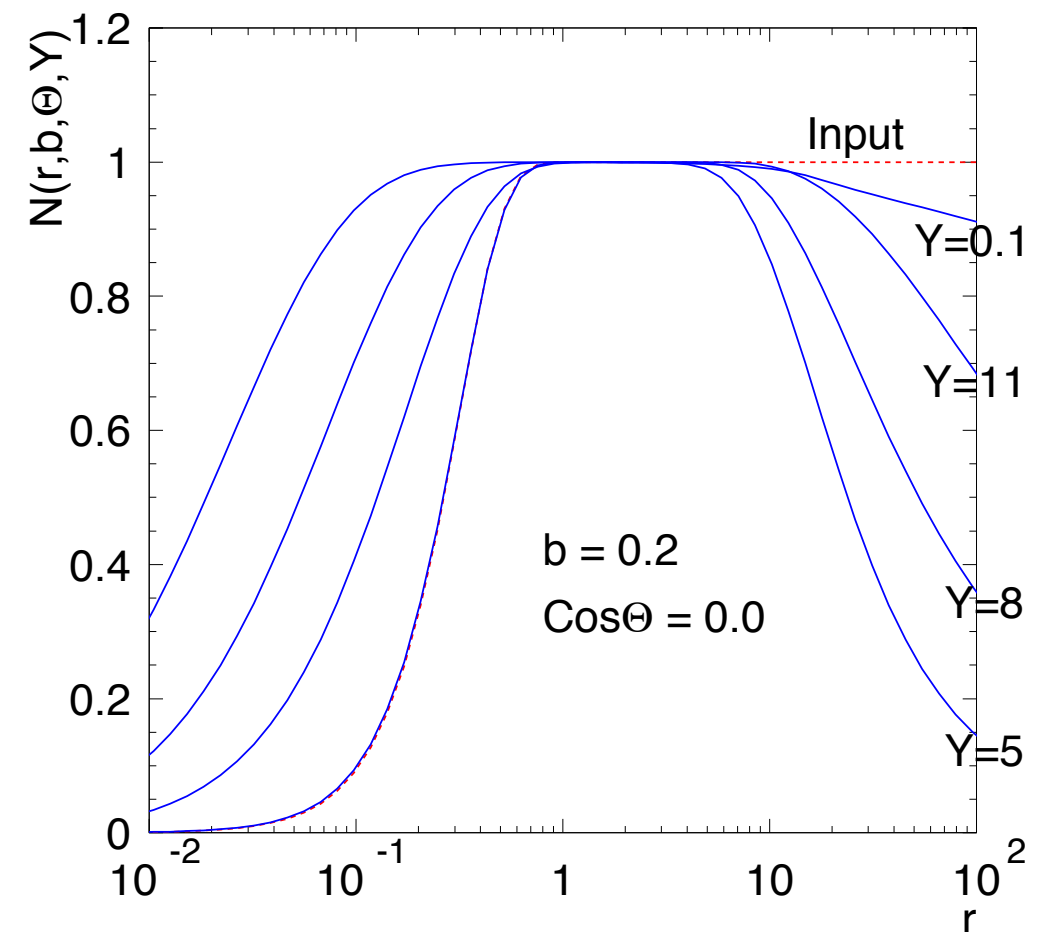
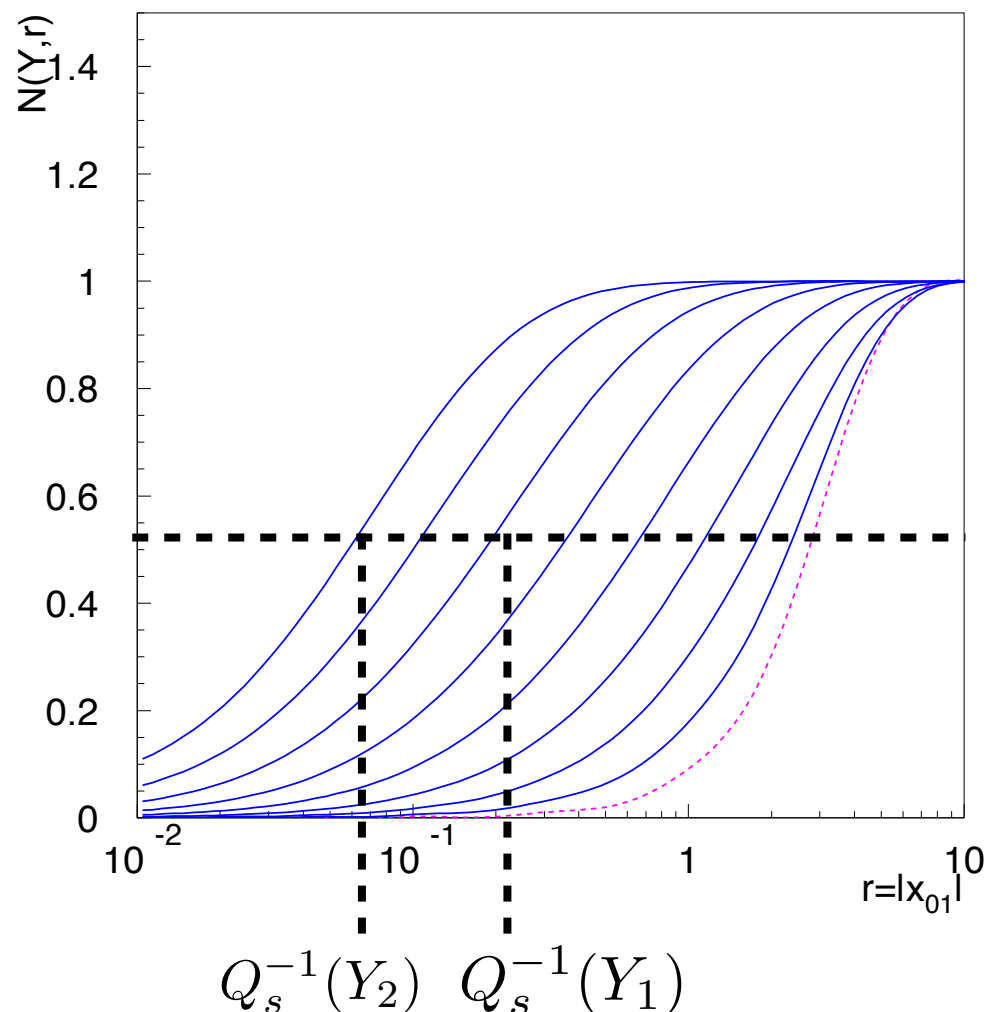
Golec-
Biernat,AS;
Berger,AS;

Initial condition Glauber-Mueller type: $N^{(0)} = 1 - \exp(-c_r r^2 \exp(-c_b b^2))$

Without impact parameter dependence

With impact parameter dependence

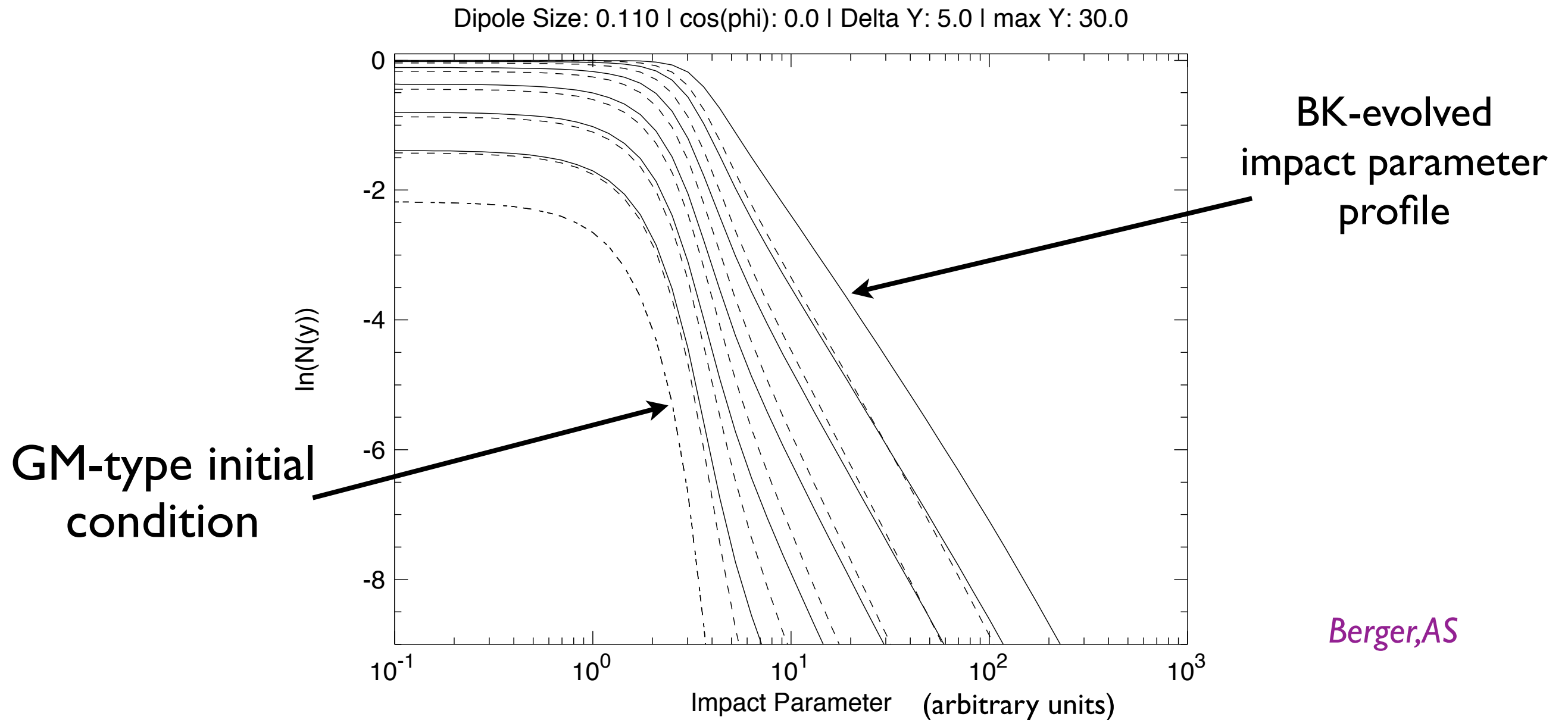
Dipole amplitude as a function of dipole size(arbitrary units)



Glauber-Mueller form is not conserved
under low x evolution

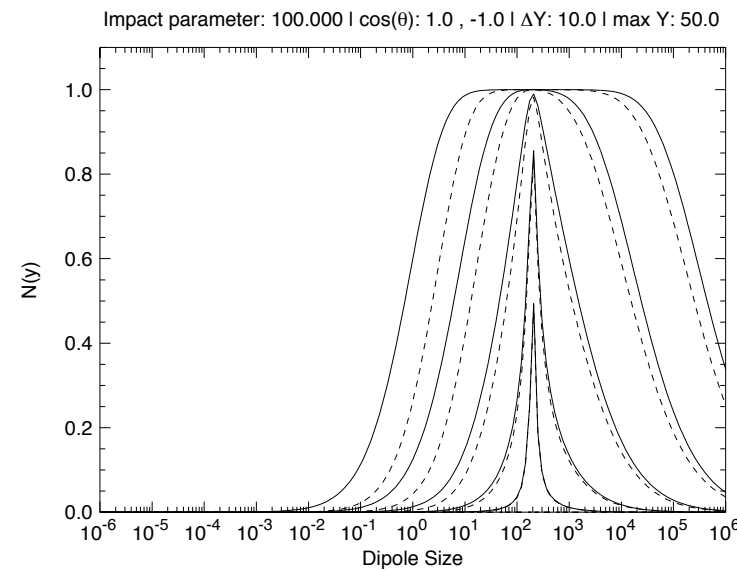
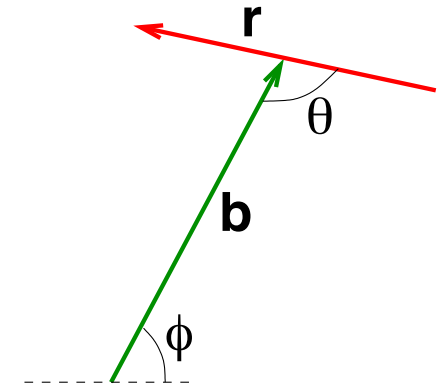
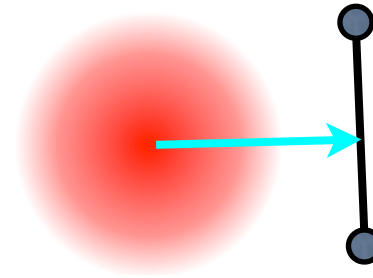
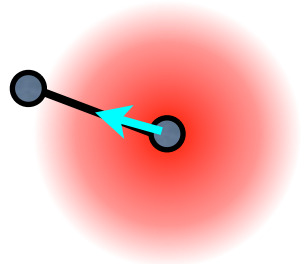
Golec-Biernat,AS

Impact parameter profile of the interaction region

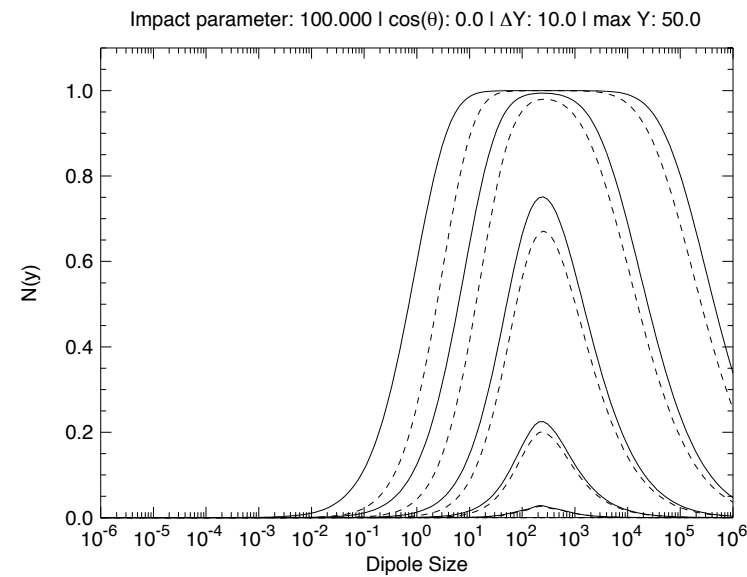


- Saturation for small impact parameters
- No saturation for large impact parameters (system is still dilute)
- Initial impact parameter profile is not preserved
- Power tail in b is generated, this is due to perturbative evolution and lack of confinement effect.

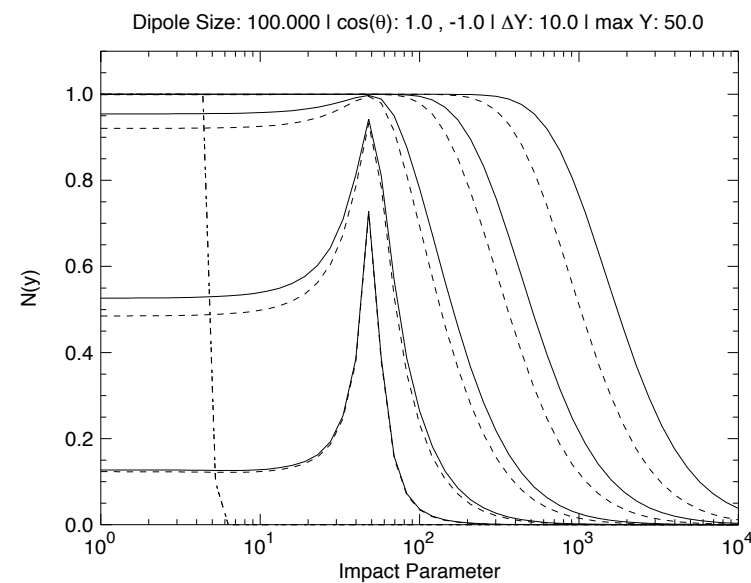
Angular correlations



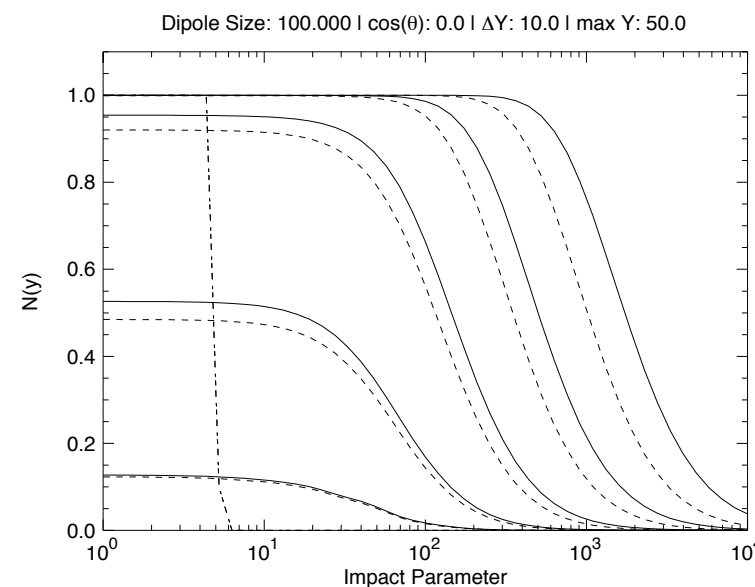
(a) $\cos(\theta) = 1.0, -1.0$



(b) $\cos(\theta) = 0.0$



(a) $\cos(\theta) = 1.0, -1.0$



(b) $\cos(\theta) = 0.0$

Angular correlations present in the solution

Amplitude larger for aligned configurations of the dipole

Could be relevant for the angular sensitive observables

Sensitivity through diffractive dijet in photoproduction/DIS

*Hatta, Xiao, Yuan;
Altinoluk, Armesto, Beuf, Rezaeian;*

Berger, AS

Initial condition and cutoff for large dipoles

At $x_0=0.01$ use Glauber-Mueller formula:

$$N(r, b, Y_0 = \ln 1/x_0) = 1 - \exp \left(-\frac{\pi^2}{2N_c} r^2 x g(x, \eta^2) T(b) \right) \quad T(b) = \frac{1}{8\pi} e^{\frac{-b^2}{2B_G}}$$

with parameters from Kowalski, Motyka, Watt $B_G = 4 \text{ GeV}^{-2}$ $\langle b^2 \rangle = 2B_G$

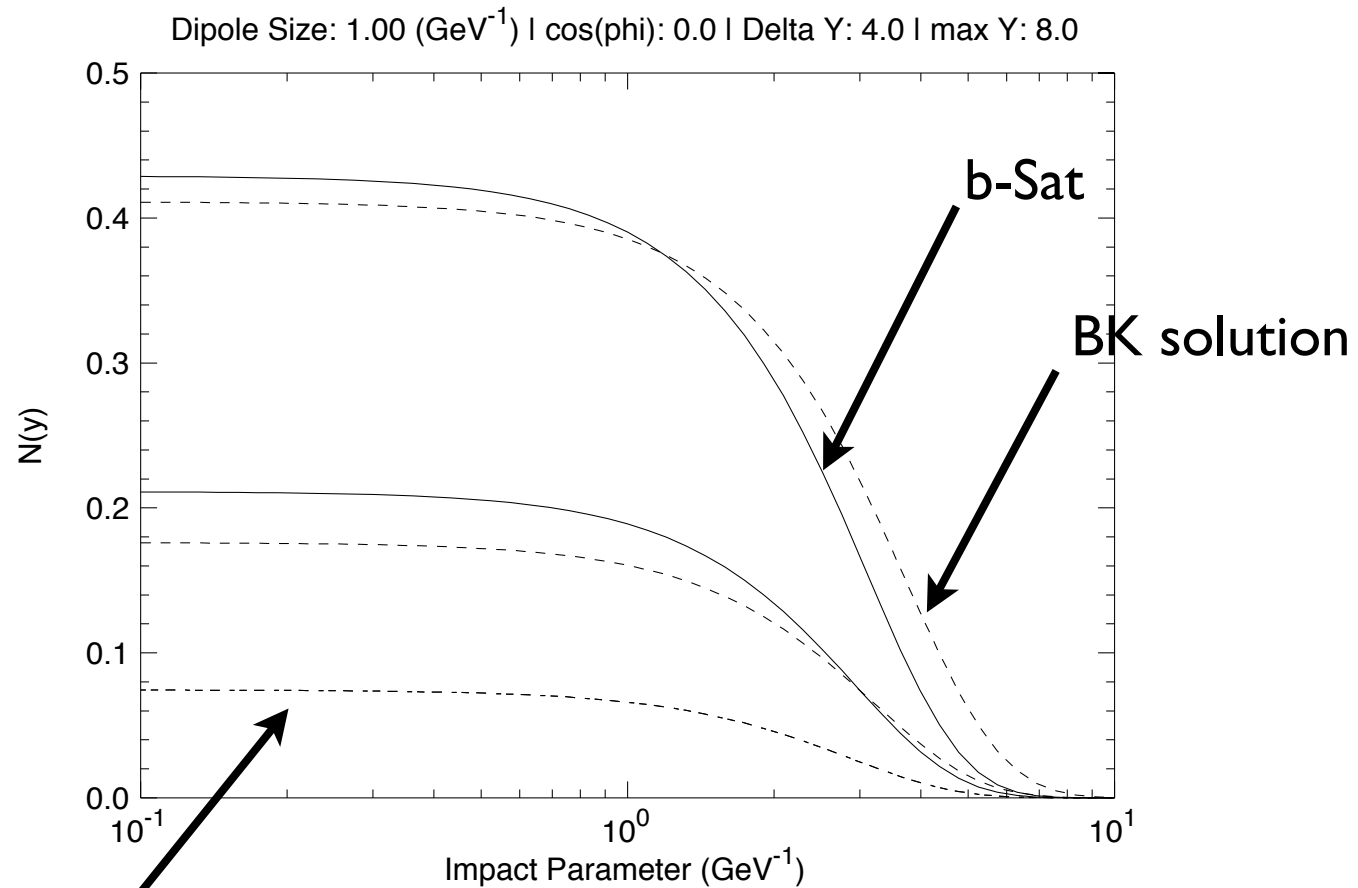
Need to implement the cutoff to regulate large dipole sizes,
mimic confinement:

$$K = dx_{02}^2 \bar{\alpha}_s \frac{x_{01}^2}{x_{02}^2 x_{12}^2} \Theta\left(\frac{1}{m^2} - x_{02}^2\right) \Theta\left(\frac{1}{m^2} - x_{12}^2\right)$$

Cutoff: $m \simeq 1/\sqrt{2B_G} \sim 350 \text{ MeV}$ $\sqrt{2B_G} \simeq 2.83 \text{ GeV}^{-1}$

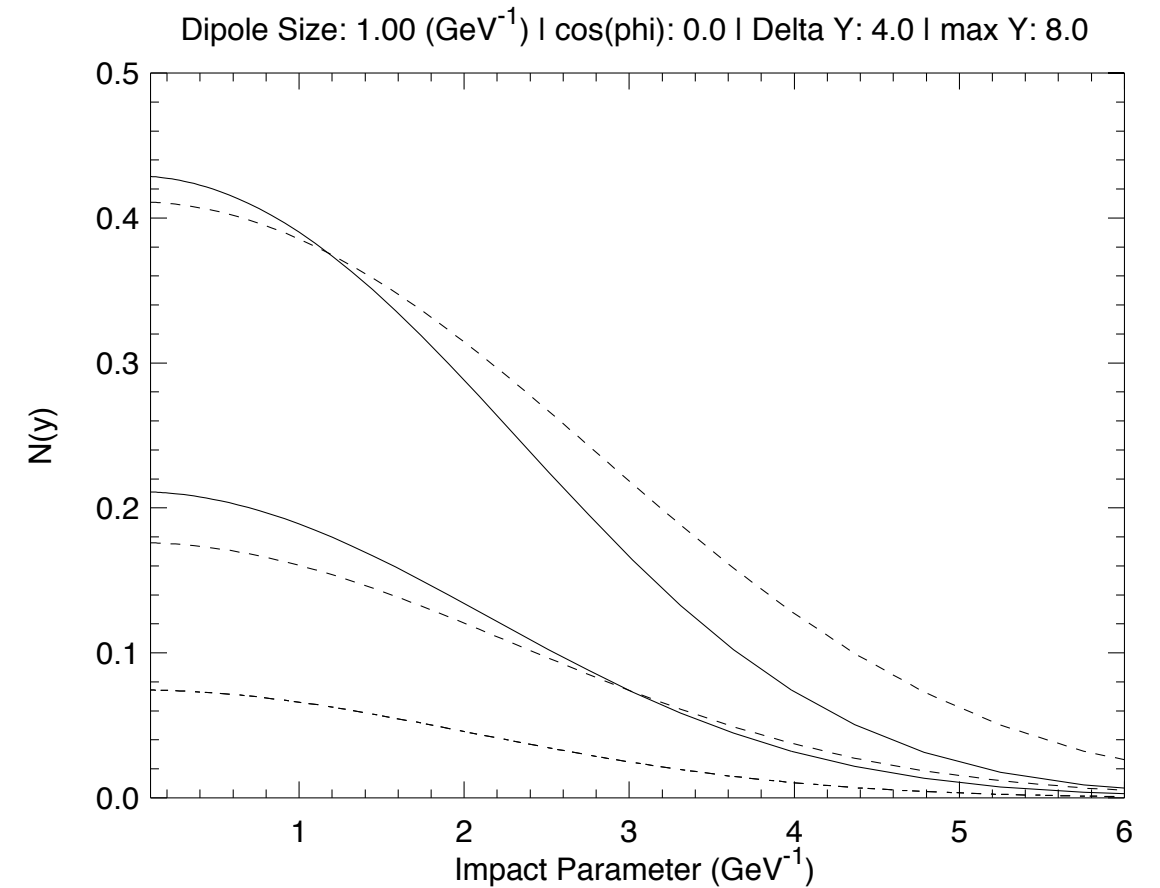
Cutoff included both in the evolution kernel and in the GM initial condition.
Refit the inclusive HERA data for F_2

Evolved solution for the dipole amplitude



KMW (b-Sat model)
initial condition

Berger, AS

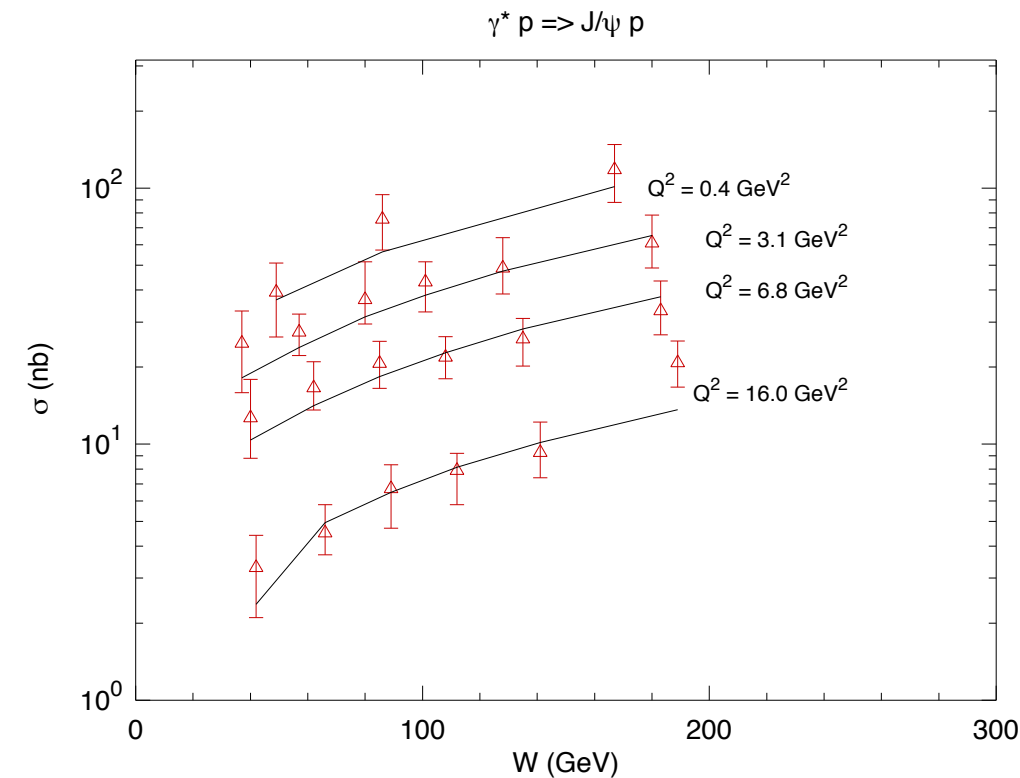
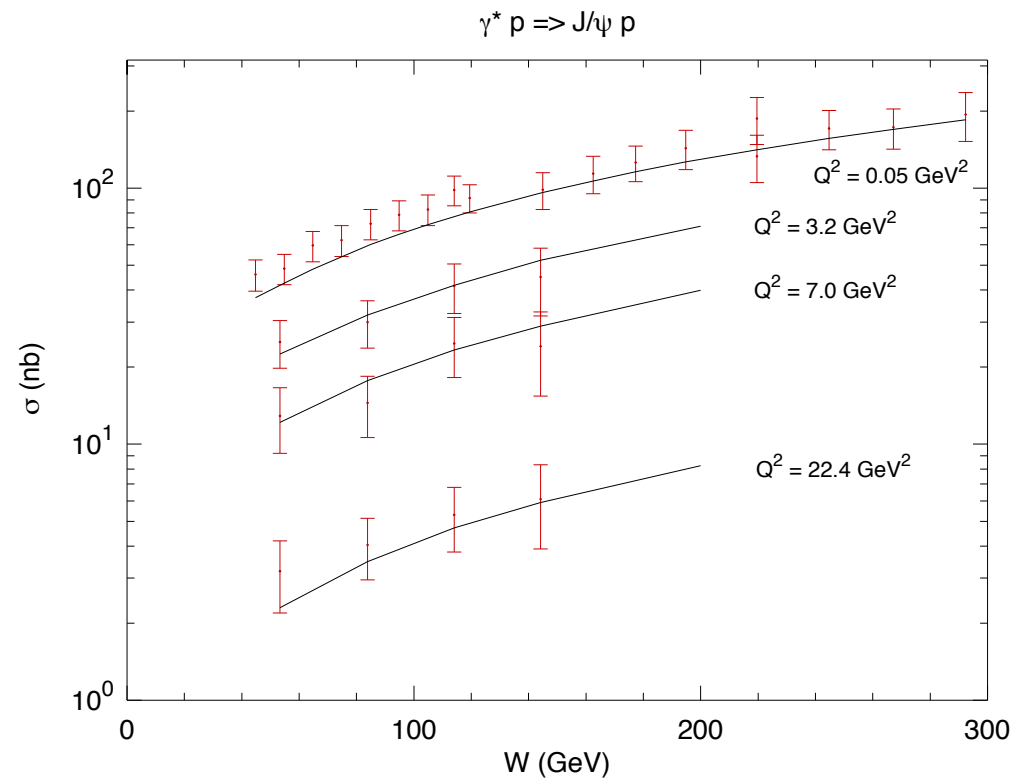


Profile in b : Solid line KMW, dashed lines BK with running coupling and cuts
Small x evolution leads to the broader distribution in impact parameter
Change of shape with decreasing x

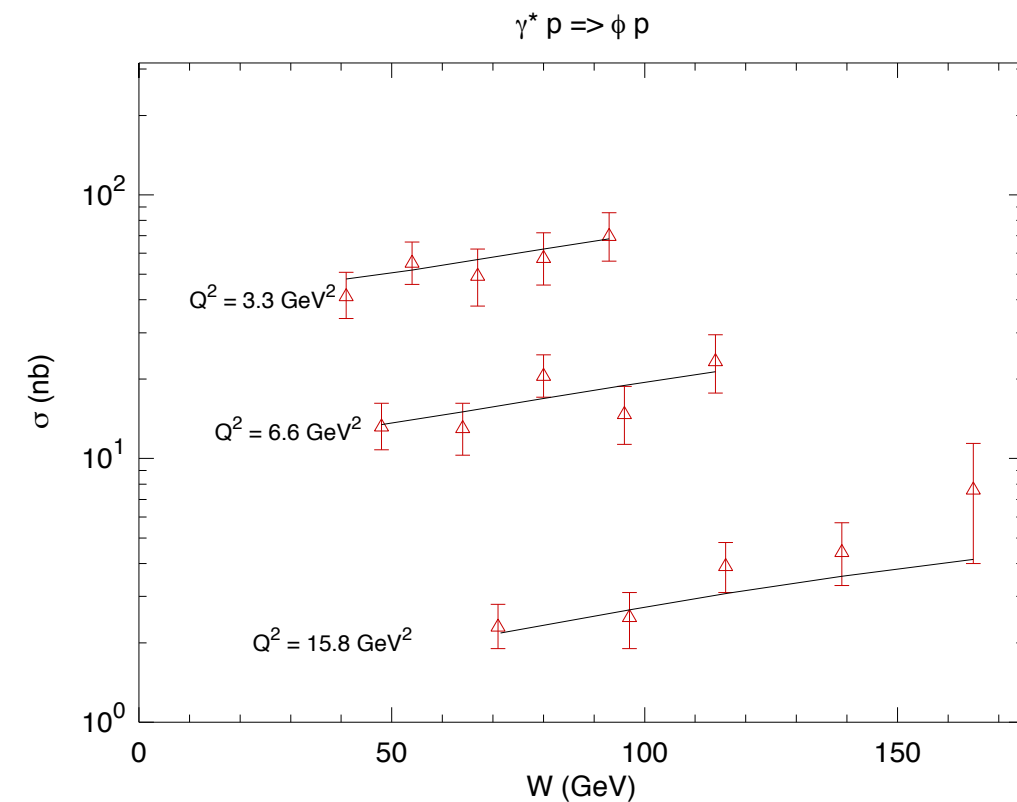
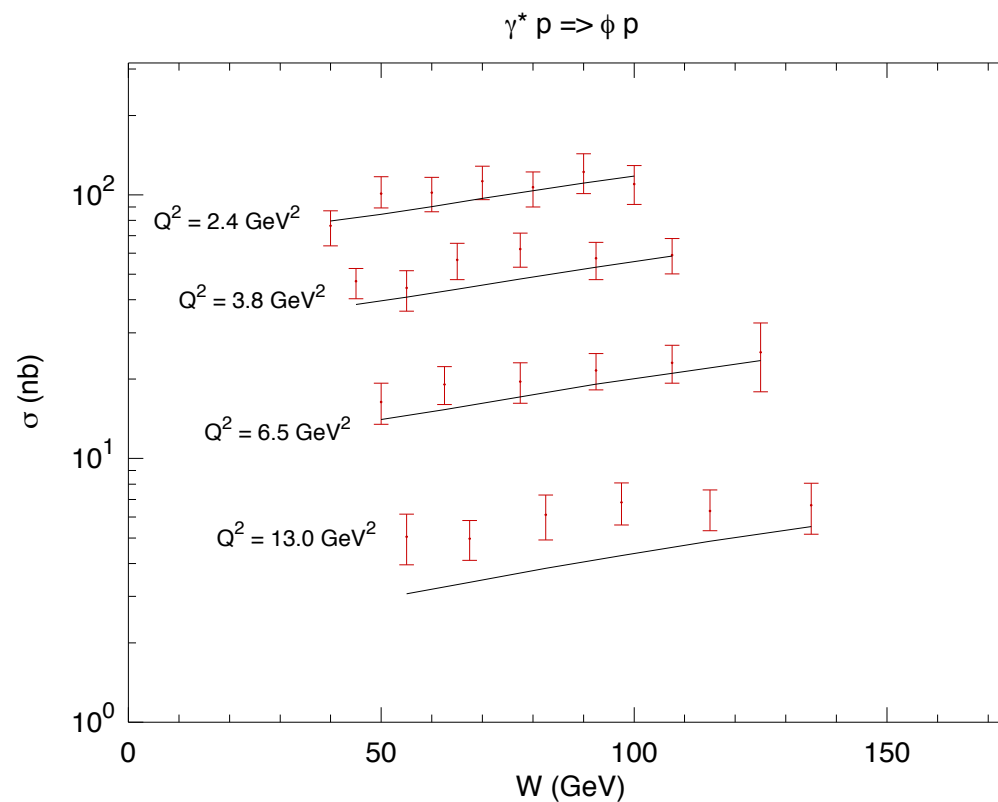
Exclusive process: photo(production) and DIS

$J/\Psi, \phi$

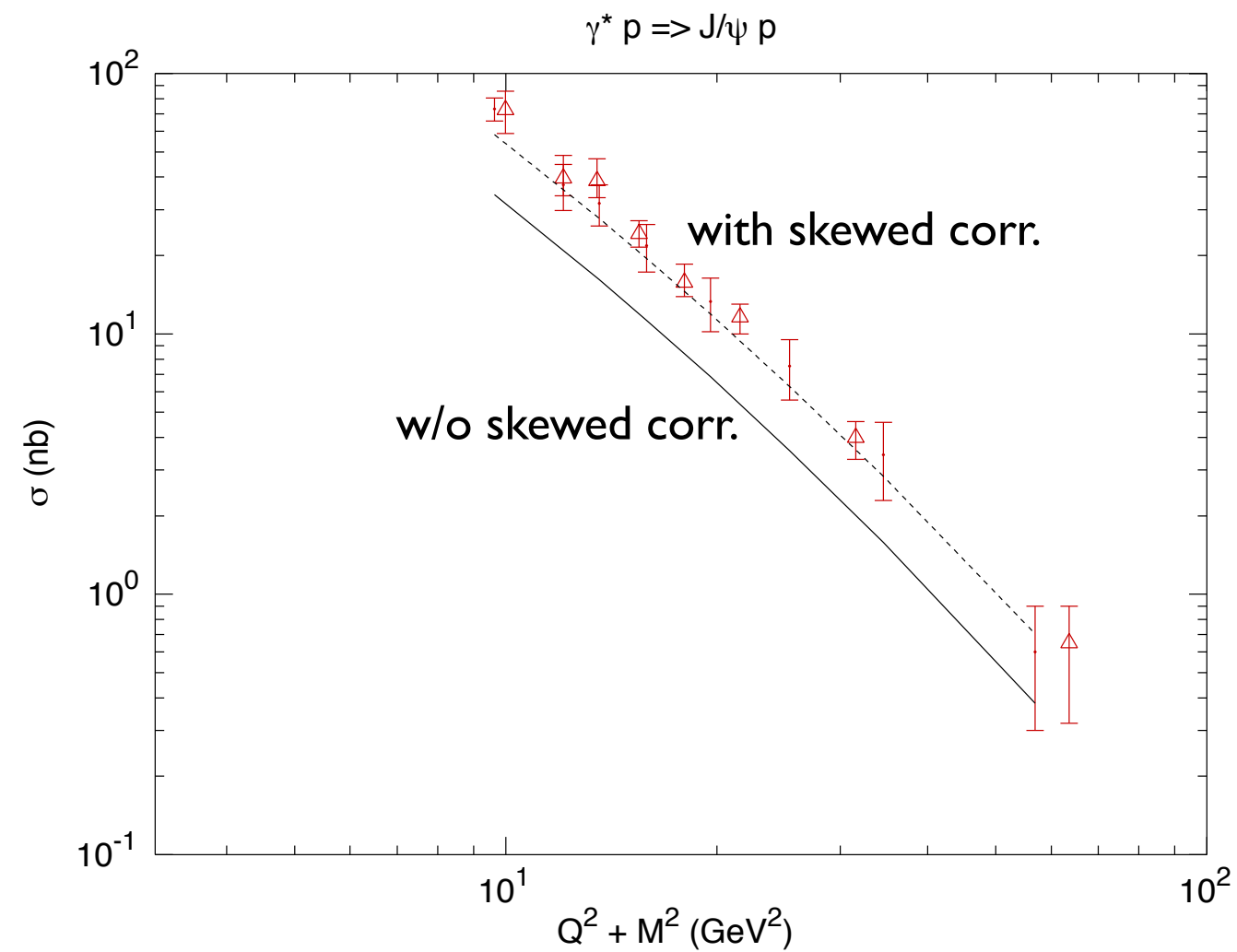
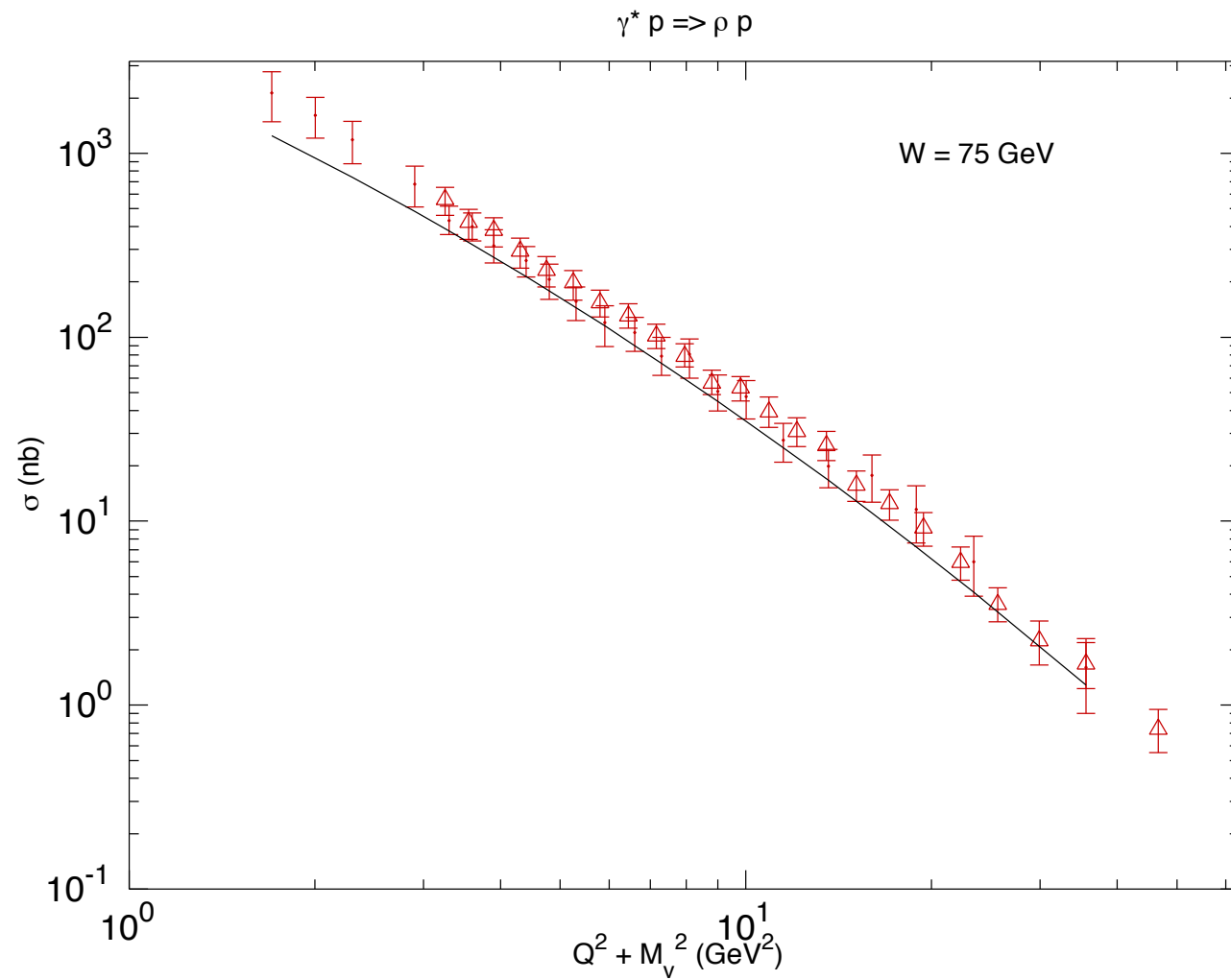
exclusive
production;
comparison with
HERA data



Integrated(over t):
good description
of the energy
dependence

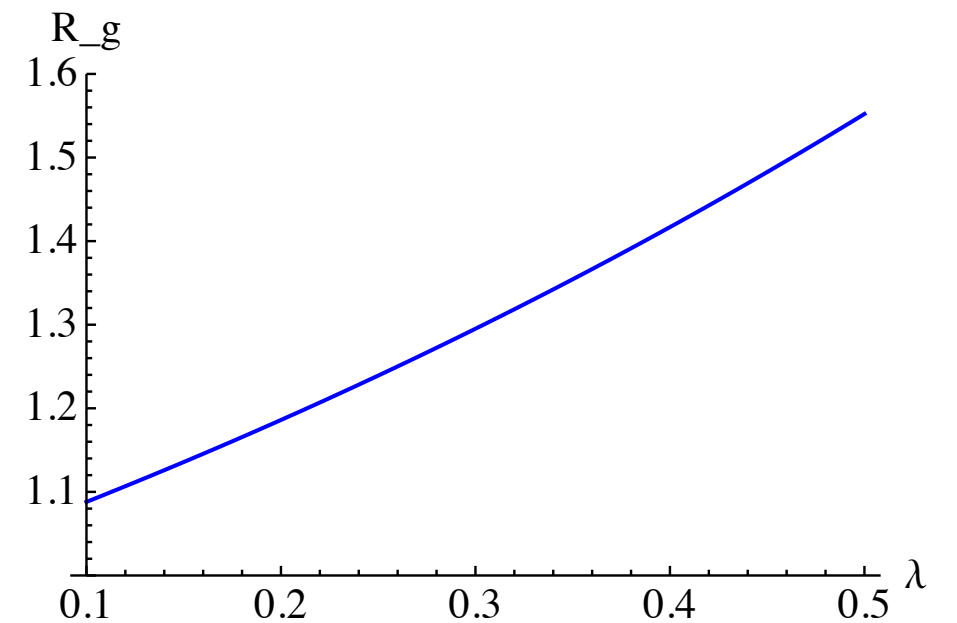


Correction from skewedness

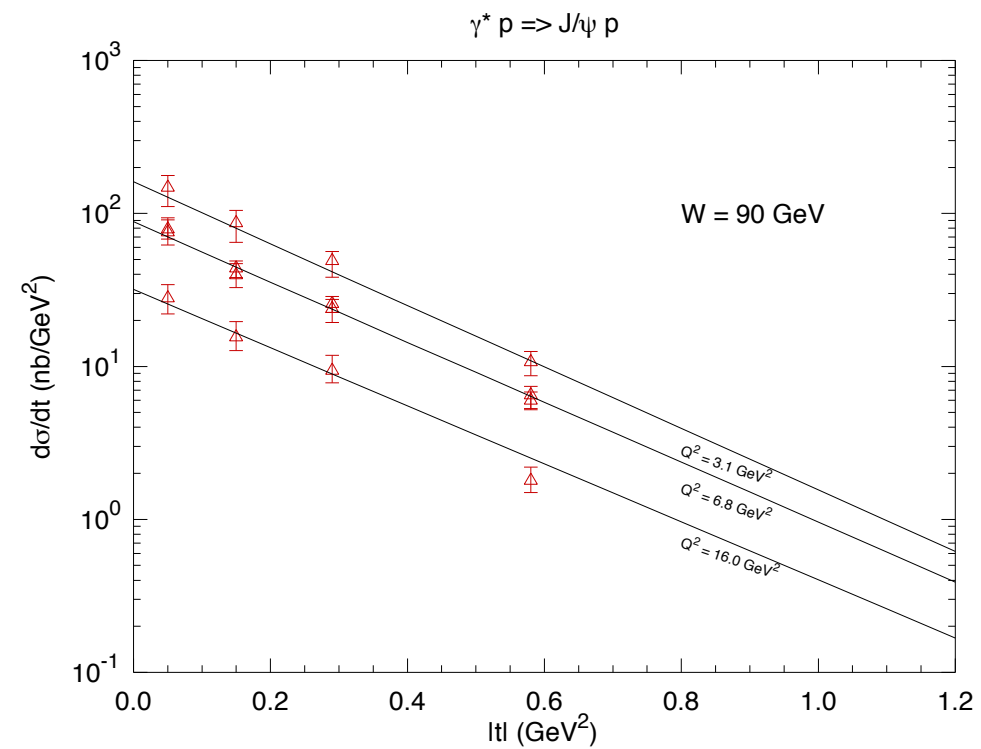
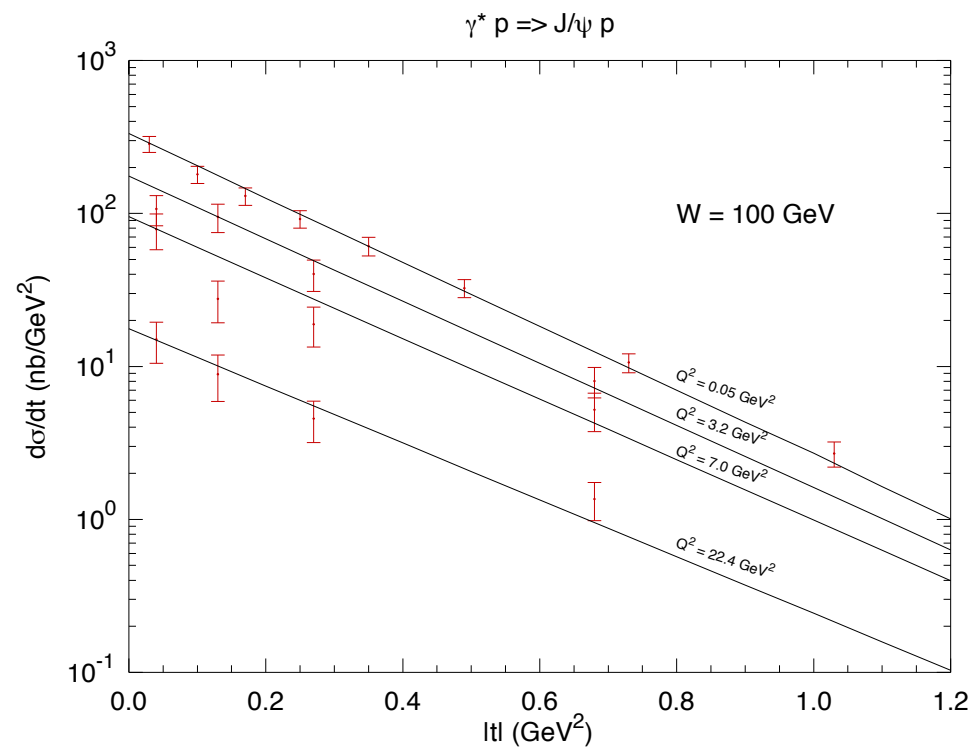
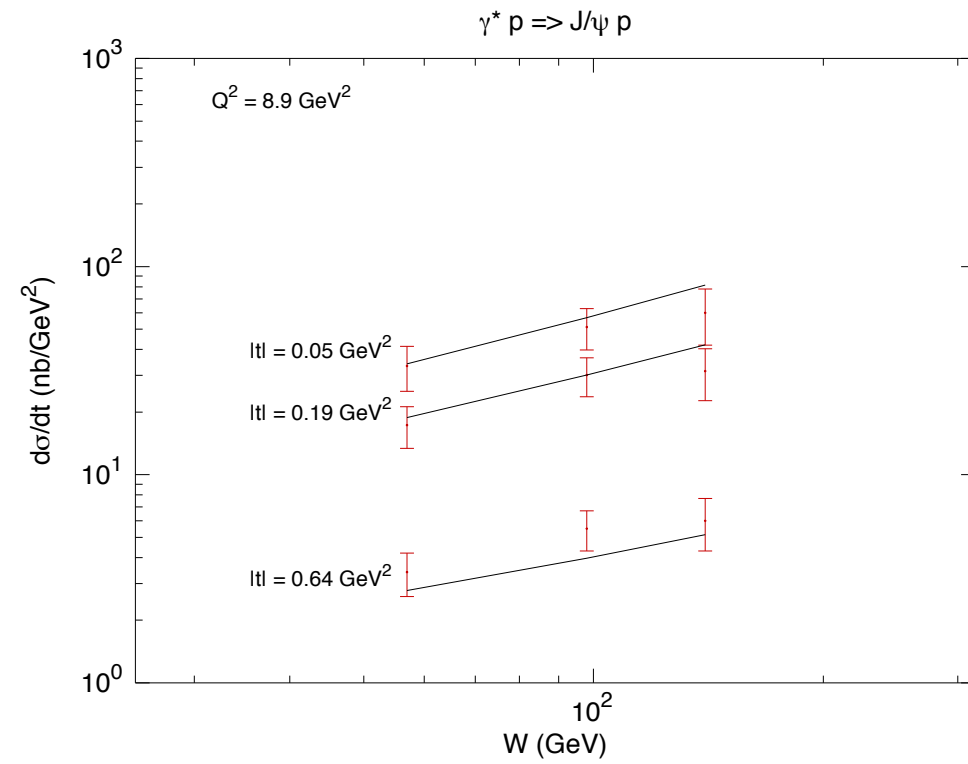
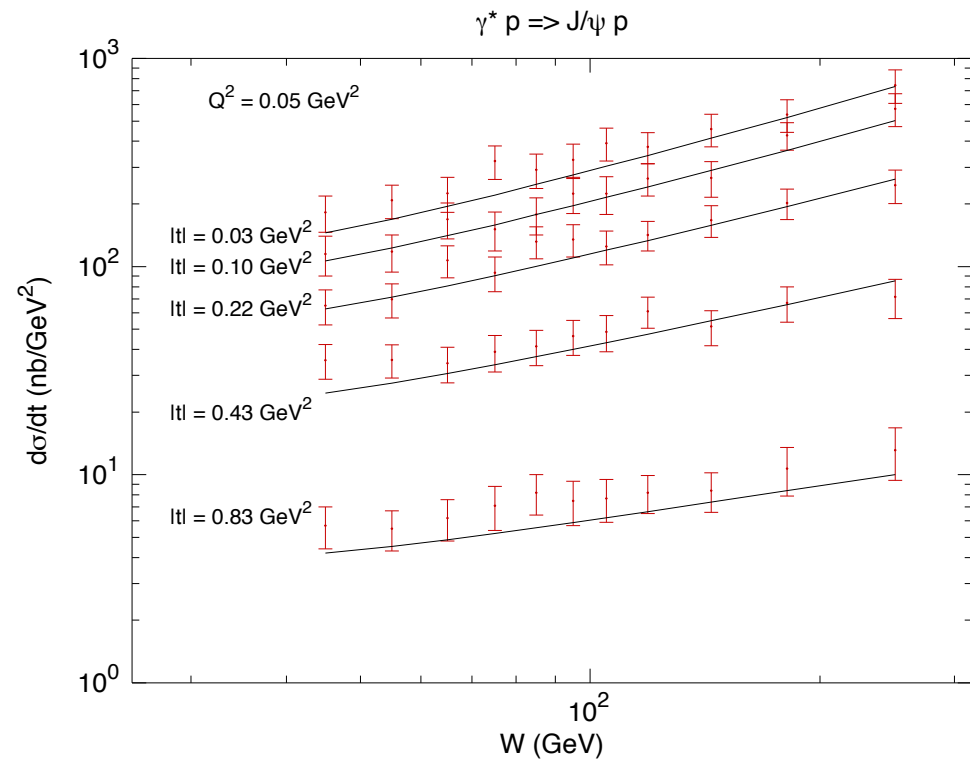


Effect of correction from skewed gluon distribution non-negligible

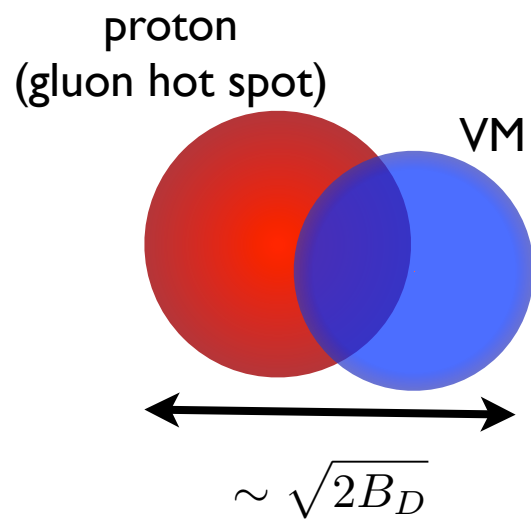
$$R_g = \frac{2^{2\lambda+3}}{\sqrt{\pi}} \frac{\Gamma(\lambda + \frac{5}{2})}{\Gamma(\lambda + 4)}$$



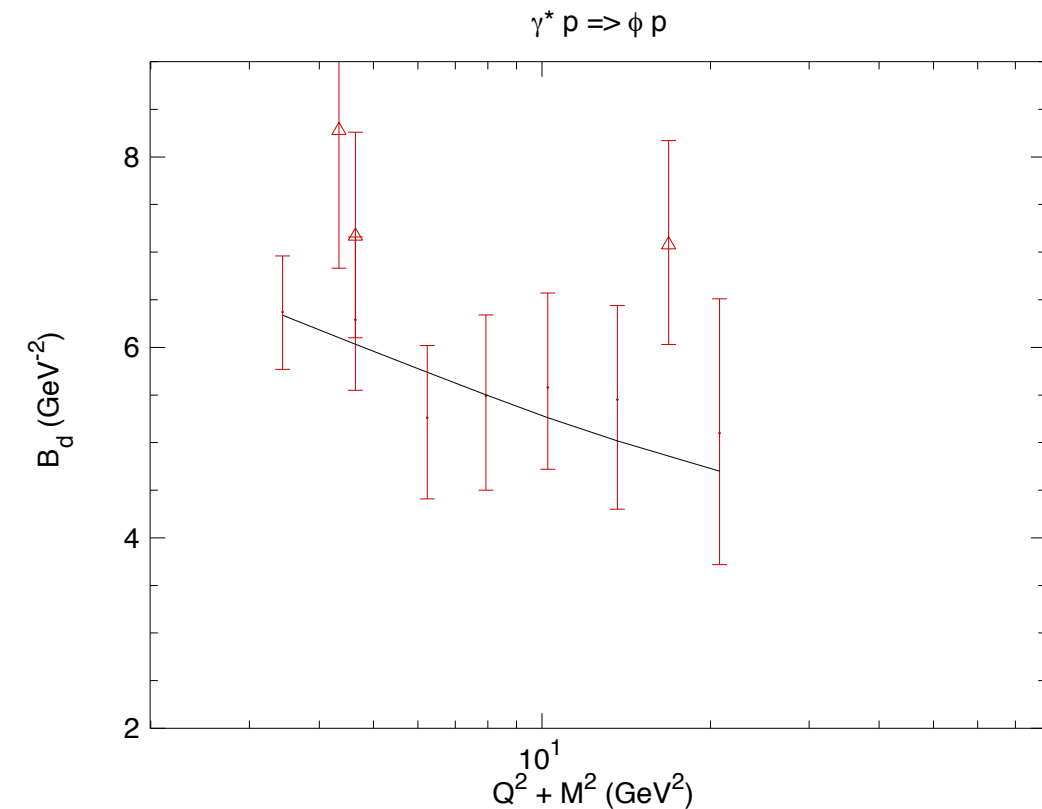
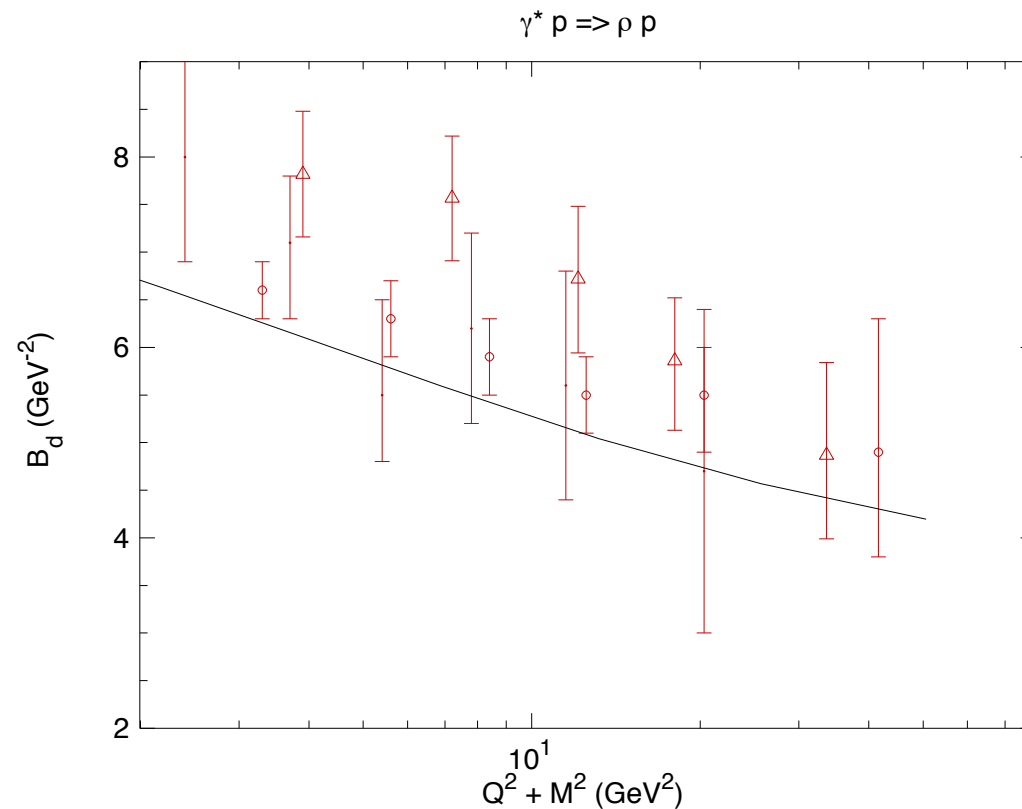
Differential cross section



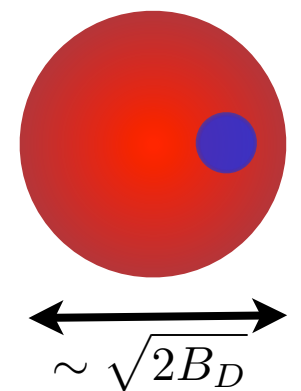
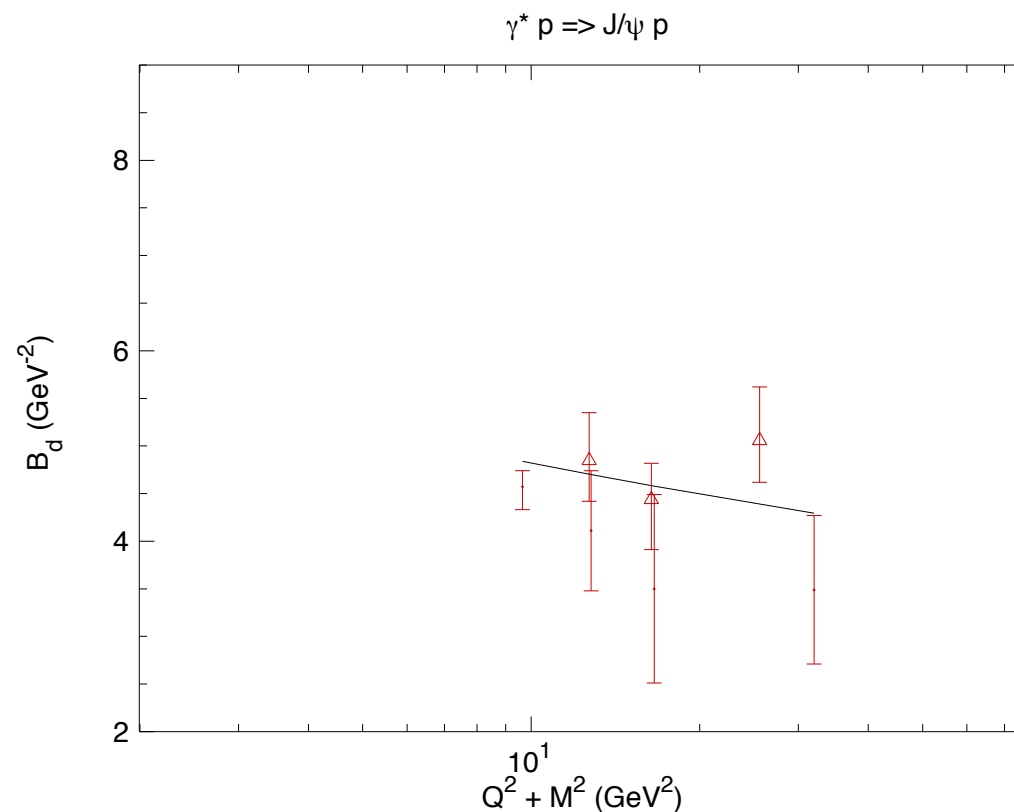
Diffractive slope



$$\frac{d\sigma}{dt} \sim e^{-B_D |t|}$$



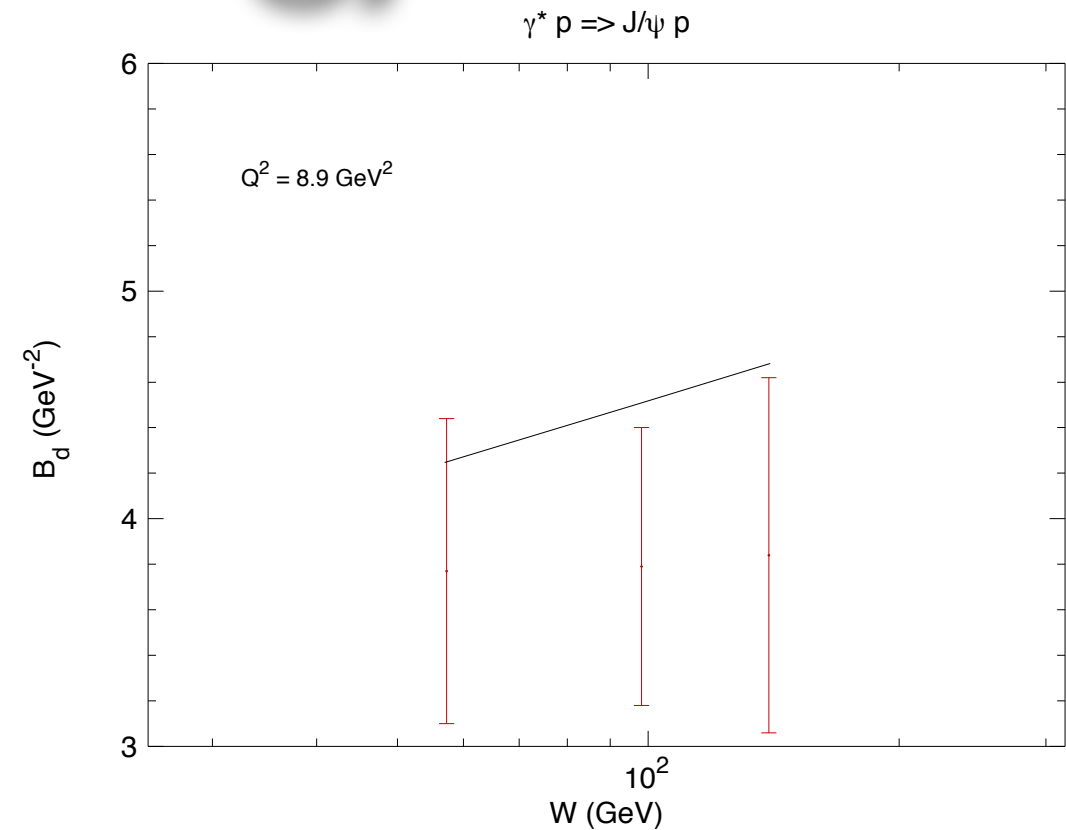
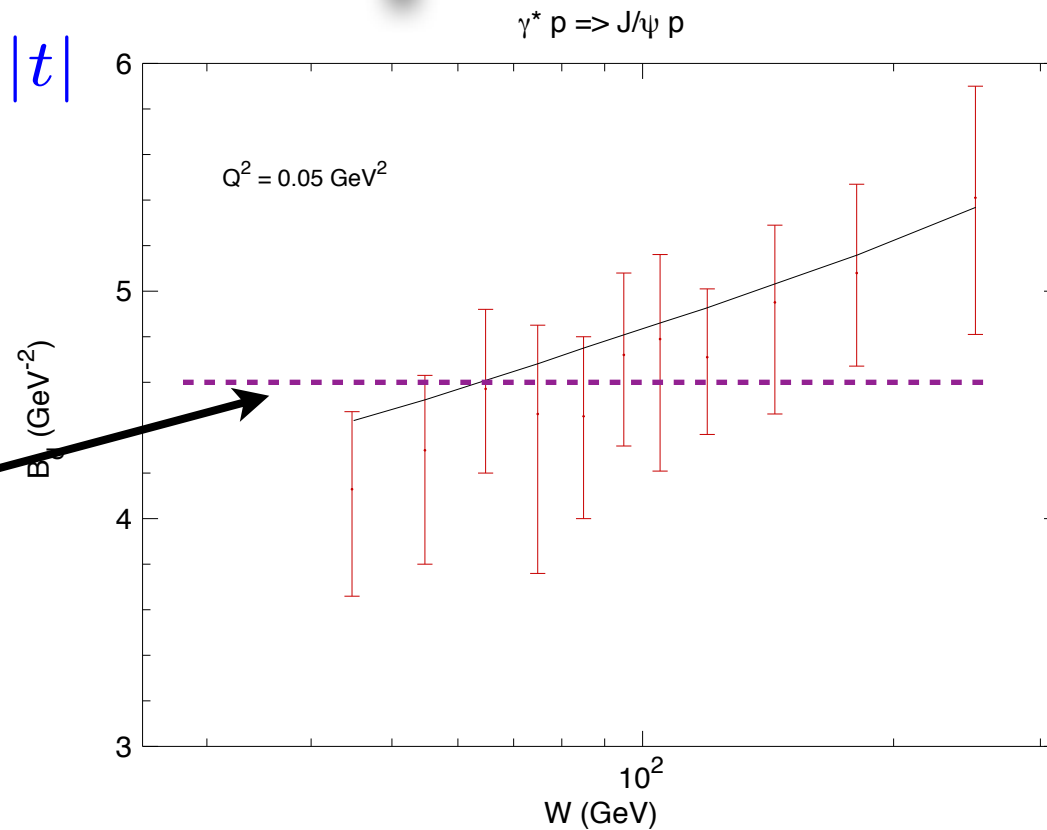
- The value of B_D is closely related to the transverse size of the interaction region which is a combination of the size of the VM and the size of the gluon hot-spot in the proton.
- In the case of the lighter mesons it is the first one which prevails.
- For heavier mesons, it is the larger size of the gluon distribution in the proton. Thus it does not depend on Q^2 that much.



Slope vs energy

$$\frac{d\sigma}{dt} \sim e^{-B_D |t|}$$

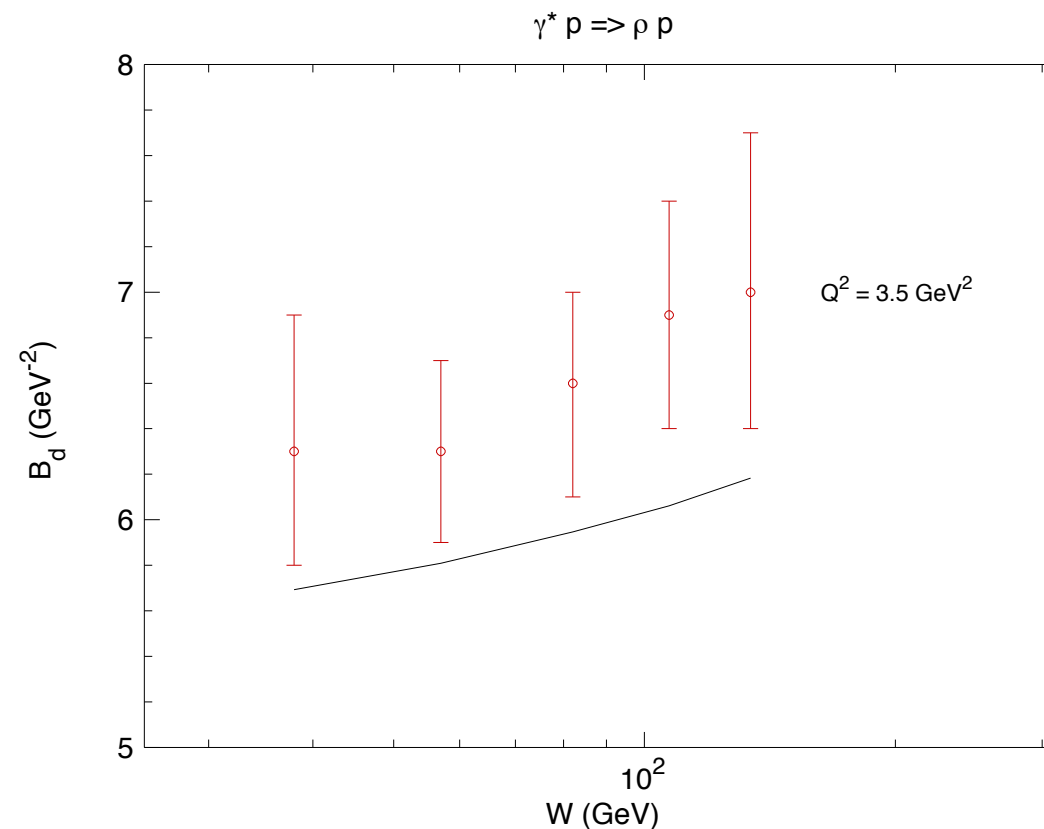
Original b-Sat model has flat dependence



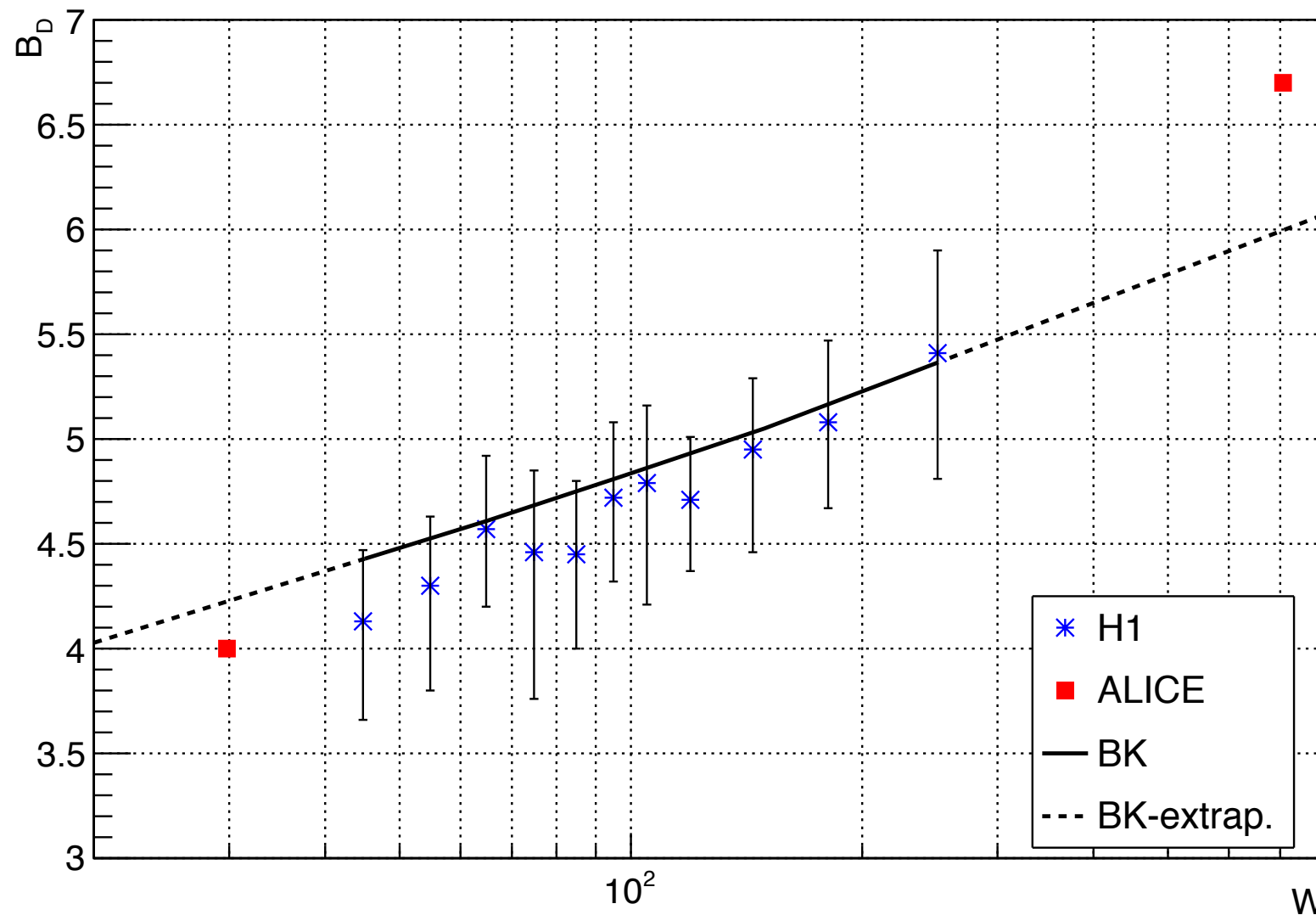
Intercept controlled by the initial profile in b, slope controlled by the mass regulator in the kernel.

Trend of the data nicely reproduced.

ρ on the lower side : more non-perturbative corrections



Slope vs energy



ALICE

$$B_D(W = 29.8 \text{ GeV}) = 4 \text{ GeV}^{-2}$$

$$B_D(W = 706 \text{ GeV}) = 6.7 \text{ GeV}^{-2}$$

- Reasonable description of the diffractive slope from dynamical prediction based on BK evolution with cutoff
- By making mass regulator smaller, the slope can be increased
- Functional dependence on energy could help determine type of cutoff: sharp or exponential

Questions for theory and experiment

- Inclusive diffraction:
 - Diffractive PDFs: future ep collider with extended kinematics can put more constraints onto DPDFs
 - Higher energy ep collider could measure precisely diffraction with heavy quarks (b,c), testing factorization in diffraction
 - Diffraction with nuclei: EIC could measure diffractive PDFs in nuclei
 - Putting more stringent limits on DGLAP evolution in diffraction; tests of onset of higher twists
 - Theory: What are the limitations on the Regge vertex factorization in diffraction? Can one do better higher twists analysis: matching DGLAP with low x/dipole model type ?
- Exclusive diffraction:
 - Energy dependence of t slope (perhaps can be done at LHC with J/ψ), but could be interesting with different VM and Q^2
 - Questions for theory: higher Fock components, better constrained VM wave functions, skewedness factor, impact parameter dependence